A TEMPERATURE-CONTROLLED GLOVE WITH NON-INVASIVE ARTERIAL PULSE SENSING FOR ACTIVE NEURO-VASCULAR ASSESSMENT

A Dissertation
Presented to
The Academic Faculty

by

Andrew Michael Carek

In Partial Fulfillment
of the Requirements for the Degree
Master in Science in the
School of Electrical and Computer Engineering

Georgia Institute of Technology
December 2016

A TEMPERATURE-CONTROLLED GLOVE WITH NON-INVASIVE ARTERIAL PULSE SENSING FOR ACTIVE NEURO-VASCULAR ASSESSMENT

Approved by:

Dr. Omer Inan, Advisor
School of Electrical and Computer Engineering
Georgia Institute of Technology

Dr. Vincent Mooney
School of Electrical and Computer Engineering
Georgia Institute of Technology

Dr. James Rehg
School of Interactive Computing
Georgia Institute of Technology

Date Approved: December 9, 2016

ACKNOWLEDGEMENTS

I would like to express my gratitude to my advisor, Dr. Omer Inan, for his continuous support and guidance. His passion and drive in the medical field has been an inspiration for me during my studies here at Georgia Tech.

I would like to thank Dr. Vincent Mooney and Dr. James Rehg for taking the time to serve on my Master's thesis committee. I would like to extend my gratitude to my fellow members of the Inan Research Lab.

Finally, I would like to thank my family for always being there with love and encouragement.

TABLE OF CONTENTS

LIST OF TABLES

LIST OF FIGURES

SUMMARY

A non-invasive, active neuro-vascular assessment system was developed using a modified temperature-controlled glove and physiological sensing. The glove incorporates local heating and cooling of the hand using multi-point skin temperature measurements as feedback, and thereby induces local and central mechanisms involved in thermoregulation. Electrocardiogram (ECG), photoplethysmogram (PPG) and non-invasive finger-cuff based blood pressure (BP) measurements were used to monitor electrophysiology and hemodynamic changes in response to temperature modulation. Then, the triggered neuro-vascular mechanisms associated with thermoregulation were quantified by extracting parameters from the measured waveforms, specifically heart rate variability (HRV), vascular tone, and BP. The system was tested on six young, healthy individuals with no history of cardiovascular diseases. During heating, vasodilation, decrease in systolic BP, and a decrease in parasympathetic tone were observed, while during cooling, vasoconstriction and increased BP were observed. While such changes are expected physiologically using passive experiments, the ability to modulate the physiology non-invasively with a controlled, quantitative, and inexpensive instrument can potentially enable serial assessments of neuro-vascular control outside of clinical settings.

CHAPTER 1. INTRODUCTION

The microvasculature comprises the smallest vessels in the body. It consists of an interplay between neural projections (i.e., autonomic nervous system [ANS] control), endothelial cells, and smooth muscle cells. The roles of the microvasculature include proper regulation of blood flow through the body to remove cell waste, regulate temperature, and delivering nutrients to the tissues [4]. The autonomic nervous system (ANS) – regulated by the hypothalamus – controls vascular tone, blood pressure (BP) and cardiac output in response to external stimuli [5]. The ANS comprises of both sympathetic and parasympathetic tone to either cause a "fight or flight" or a "rest and digest" response [6]. The more local elements of regulation, the endothelium, directly regulate vascular tone by the release of certain enzymes [7]. The endothelium, along with the sympathetic nerve fibers, direct these signals to the smooth muscle cells to cause either vasoconstriction or vasodilation.

The microvasculature has received great attention due to the association of its dysfunction with many cardiovascular diseases and neurodegenerative disorders. In some instances, such as type 2 diabetes, microvascular function can degrade slowly over time [8]. Accordingly, it can be beneficial to allow longitudinal, accurate monitoring of microvascular health outside of clinical settings to allow the state of such patients' health to be closely tracked. Such assessment of microvasculature can also be considered a means of monitoring neuro-vascular health due to the complex interplay between neural control (i.e., ANS) and vascular modulation (i.e., vasodilation / vasoconstriction) that are required for its normal function.

1.1 Motivation

Currently, there are no convenient techniques for assessing microvascular health outside of a lab setting without specialized personnel. Coronary angiography is able to directly analyze impairments in endothelial mechanisms though images. However, an injected contrast agent is needed, making the procedure invasive and clearly confined to hospital / clinic settings only [9]. A commonly used technique for microvascular health assessment is flow-mediated vasodilation. A shear stress is applied to the brachial artery and the ability of the arteries to dilate is measured. This procedure is also unrealistic for at-home use due to the bulkiness of the hardware and the requirement for a trained sonographer to administer the test [10]. Finger plethysmography is able to quantify the changes in vascular tone by measuring blood flow after the occlusion of the brachial artery, but may be evaluating different aspects of vascular biology [11].

The responsiveness of the microvasculature to heating and cooling of the skin may potentially provide a window to examining the health of this system. At a local level, upon exposure to a cold environment, skin blood flow decreases due to vasoconstriction of these small vessels, due to chemicals released by endothelial cells [12]. The decrease in blood flow reduces the heat dissipation from the skin surface [13] and an increase in vascular resistance during cooling also results in an increase in mean arterial pressure (MAP) [14]. A near opposite effect occurs with heat exposure: local vasodilation (also mediated by the endothelium) results in an increase in blood flow to maximize the heat transfer to the environment, and vascular resistance decreases resulting in a slight decrease in MAP. If the change in temperature is sufficient to trigger a more central mechanism, high frequency heart rate variability will increase [15, 16], indicating a decrease in parasympathetic

activity and an increase in sympathetic activity. Thus heating and cooling of the skin can lead to both local responses (triggered by release of chemicals by the endothelium and the corresponding contraction / relaxation of the smooth muscles) and central responses (based on changes in parasympathetic / sympathetic tone in the ANS).

Currently, the cold pressor test is a common technique to stimulate neuro-vascular mechanism by immersing a hand into an ice bucket; however, it can be difficult to differentiate the effect of the cold pressor and an external stimuli such as pain or touch [17]. This makes it challenging for cold pressor to consistently modulate the different mechanisms related to the temperature gradient. Any initial impact of either the cold or heat may unintentionally also alter hemodynamics. In addition, visual or auditory stimuli may have an effect on ANS responses with cold and heat exposure [15]. To more accurately measure the changes in the microvasculature, these external stimuli should be limited. More importantly, a cold pressor test requires the attention of a trained person. Since the person undergoing the test is unable to move to prevent any neuro-vascular changes, a second person has to be present to apply the cooling/heating element. This may prevent any long-term monitoring of neuro-vascular health that could provide insight into early signs of a neuro-vascular dysfunction.

1.2 Proposed System

Much of these challenges can be handled by developing a modified temperature-controlled glove, with closed-loop feedback enabling precise control of skin temperature and the subsequent measurement of physiological responses. Thermoelectric coolers could

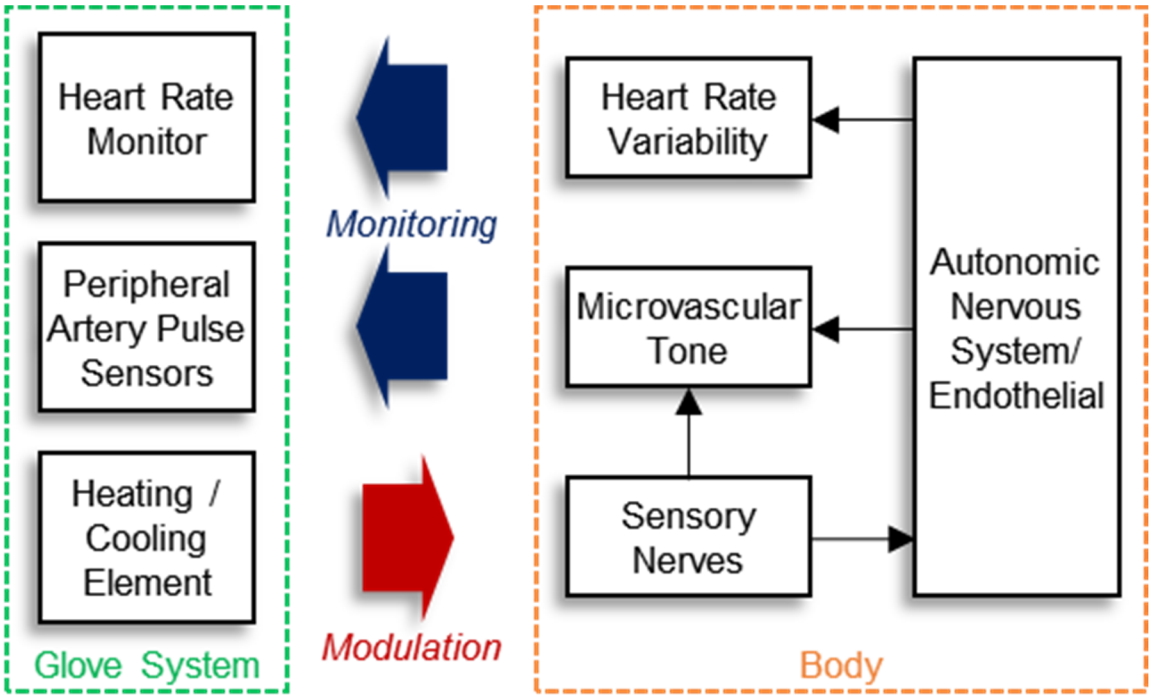

Figure 1 – Block diagram of the novel wearable system for non-invasive and active assessment of neuro-vascular health. The system consists of a heating/cooling element that actively modulates the vascular tone, and sensor that monitors the resultant change in hemodynamics and local blood flow.

be inserted into the glove to utilize the Peltier effect, allowing for heating and cooling of the glove with no moving parts. The glove can be controlled automatically through a microcontroller to regulate the temperature and to allow for minimal human interference. The only outside human element would be to start the test, a task that can be easily handled by the user. Due to the low efficiency during cooling, a challenge will present itself when attempting the remove heat from the system. Heat sinks and an intake system will need to be implemented to prevent overheating and to allow the glove to properly cool the hand.

To allow for automatic assessment of microvascular health, a temperature-controlled glove was designed and built. A polyester athletic glove was initially used both to house the components and to provide a layer of thermal insulation. Thermoelectric coolers (TECs) known as Peltier tiles were used to modulate the temperature of the glove.

These tiles utilize the Peltier effect to achieve a temperate gradient between the two tiles with an applied voltage [18]. The sign of this gradient is dependent on the direction of the current flow, allowing for both heating and cooling of the hand.

Six subjects were recruited to partake in the study (4 male and 2 female, Age: 23±2 years). The purpose of this study was to validate the glove's effectiveness in producing a repeatable physiological response. Electrocardiogram (ECG), both finger photoplethysmogram (PPG), and blood pressure (BP) were continuously monitored during the study. The subjects were seated in a quiet room and were asked to remain still for the entirety of the study. The glove was placed on the subject's hand and rested for four minutes. This allowed the subject to reach homeostasis and lets the glove to establish the baseline temperature. The glove then transitioned to a heating phase where the temperature rose to 9º C above the baseline temperature for 3 minutes. After a quick cooling phase to transition the temperature back to the baseline and three minutes of rest, the glove cooled the hand 9º C below the baseline. This again lasted three minutes followed by a quick heating phase to raise the temperature back to baseline.

Signal processing techniques were used to extract PPG peak-to-peak (PTP), high frequency heart rate variability (Hf HRV), the ratio between low and high frequency heart rate variability (Lf/Hf HRV), systolic blood pressure, and diastolic blood pressure. During the heating phase, the amplitude of the PPG waveform increased by an average of 14%, indicating an increase in blood volume to the hand and vasodilation. The opposite effect was found during the cooling phase with a decrease in the PPG PTP. The more central mechanism, Hf HRV, shows a 20% decrease during heating intervention. Though Hf HRV has been shown to decrease during previous cold interventions, there were no consistent

changes during this study. The final parameter with statistical significance, systolic BP, showed an increase in blood pressure during heating and cooling. These results indicate modulation in both central and local mechanisms and confirm the validity and feasibility of using a glove-based system to assess neuro-vascular health.

Figure 2 – The temperature-controlled glove is able to modulate the skin temperature with a heating and cooling element. Sensors, such as the PPG sensor shown, quantify the physiological responses.

CHAPTER 2. BACKGROUND

The microvasculature comprises the smallest of blood vessels, typically less than 150 μm in diameter, include arterioles, venules, and capillaries [5]. The microvascular system facilitates the direct interaction between the circulatory system and tissues throughout the body. Its primary role is to regulate blood flow throughout the body to respond to inflammation, provide nutrients to the tissues, achieve thermoregulation, and expel cell waste [4].

2.1 Microvasculature's Role in Regulating Blood Flow

Blood flow to the microvasculature is modulated significantly in daily life, based on real-time change to the microvascular tone, or the diameter of the blood vessels. During intense exercise, the microvasculature can increase muscle blood flow nearly 100-fold [4]. While blood vessels throughout the body contain many of the same anatomical structures, the prevalence of different layers can vary between types of vessel. On the outmost layer, a tough wall of connective tissue protects the integrity of the vessel. These comprise a large amount of extracellular matrix and are mostly found in the larger arteries and veins [19]. Vascular smooth muscle (VSM) cells form the medial layer and are responsible for the production of the extracellular matrix found in the outermost layer. Larger arteries have a thick layer of VSM, which decreases along the vascular tree as the vessel's diameter decreases. VSM are very susceptible to mechanical stress and various molecules that induce responses, allowing for a variable contractile tone to regulate the blood pressure and flow [20]. The innermost layer consists of a fine sheet of endothelial cells. Capillaries and sinusoids only an endothelial layer and a basal lama for structure. The endothelium cells play a vital role in the microvasculature, dictating the passage of material and sending signals to surrounding tissue [19].

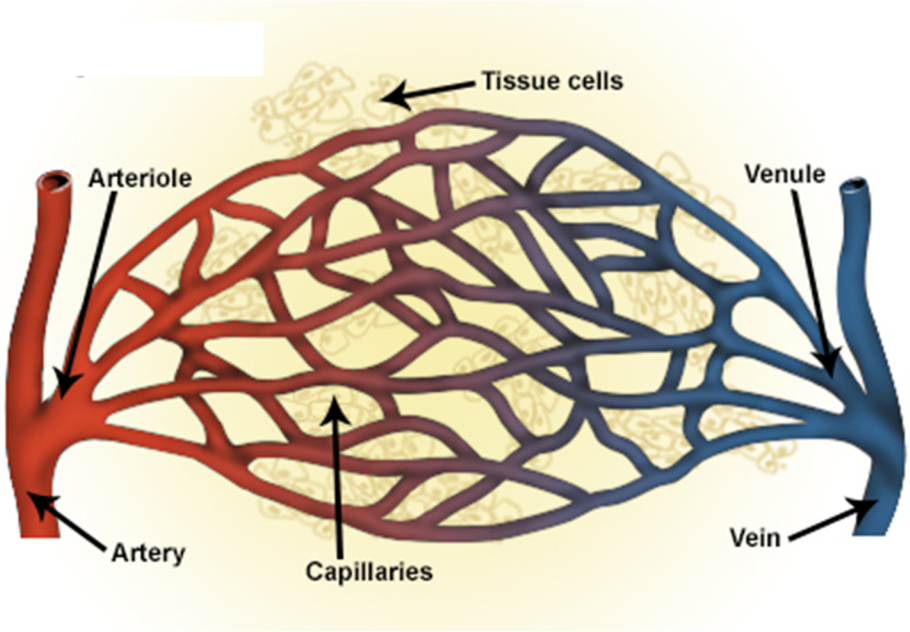

Figure 3 – As blood flows through arteries, it enters the microvasculature, comprising of the arterioles, capillaries, and venule. In [21], used with permission.

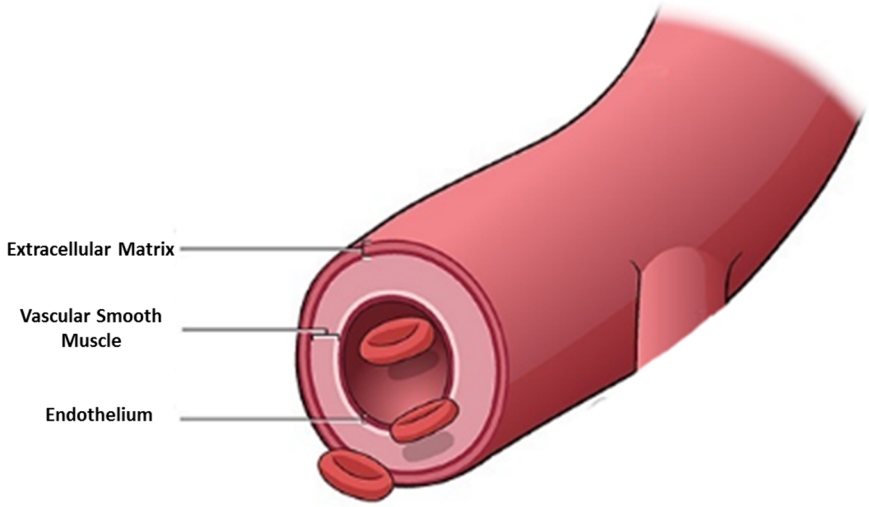

Figure 4 – The vessel wall is mainly composed of a tough outer extracellular matrix, vascular smooth muscle layer and an endothelial layer. In [22], used with permission.

2.1.1 Blood Flow Modulation

Mediation of vascular tone is regulated by either the release of nitric oxide (NO) from the endothelium or a direct induction of electrical signals to target VSM to induce vasodilatation or vasoconstriction [23]. NO is the dominant factor involved in the relaxing response of the VSM. As the compound is released, VSM increases the concentration of cGMP and causes a hyperpolarization of smooth muscle to dilate the vessel [24].

A number of factors can influence this release of NO from the endothelium including mechanical stimulation of vessels, metabolic responses, and autonomic nervous stimuli [25]. Mechanical stimulation can occur with a change of blood pressure or shear stress. To contract the vessels, myogenic response is activated with the stretching and increased tension of the vessel wall caused by the increase in blood pressure. This is important for areas in the body such as the kidneys where blood flow needs to be constant regardless of pressure [25]. With an increase in blood flow, shear stress on the innermost endothelial layer increases and flow-induced vasodilation occurs. Nitric oxide is released to relax the VSM resulting in a minimal change in blood pressure [24]. Increases in metabolic activity of the parenchyma can trigger dilation within arterioles. Evidence suggest that there may be communication between venules and adjacent arterioles to provide a feedback system for modulation of vascular tone depending on local metabolic conditions in the capillary and post-capillary regions [26].

A more direct control of the microvasculature comes from autonomic nervous system (ANS) stimuli. This system receives both external environmental and internal body signals and responds by either stimulation or suppression of bodily functions. Sensory signals are transmitted to the homeostatic control centers located at the hypothalamus and brain to modify the activation of autonomic neurons [27]. The ANS is divided into two branches, the sympathetic and parasympathetic nervous system. The constant interplay and

regulation between these systems is responsible for maintaining normal functions. The sympathetic nervous system originates from the thoracic and lumbar region of the spinal cord. Modulation of sympathetic tone is responsible for activation of function and is known as the "fight or flight" response. The parasympathetic system, stemming from the sacral region of the spinal cord is termed the "rest and digest" system and maintains normal homeostasis [28]. Both branches rely on neurotransmitters to transmit signal, most commonly acetylcholine and norepinephrine. Both the parasympathetic and sympathetic system have nerve fibers, known as cholinergic fiber, that release acetylcholine. Only the sympathetic releases norepinephrine through fibers referred to as adrenergic fibers and noradrenergic fibers [27].

The ANS is responsible for much of the control of the microvasculature, but mostly through the sympathetic branches. While parasympathetic tone has an effect on the heart and a small number of blood vessels, sympathetic nerves have a larger control of cardiac and vascular function, innervating the heart, blood vessels, adrenal glands, and kidneys [29]. In most arteries and arterioles, postganglionic sympathetic nerve endings are attached to the adventitial-medial border. Capillaries and venules lack VSM, thus are not directly innervated by sympathetic nerves. α_1 and α_2 adrenergic receptors located on the VSM are responsible for receiving the neurotransmitters released from the sympathetic nerve endings. The primary neurotransmitter is norepinephrine with increases in sympathetic outflow leading to vasoconstriction and a decrease leading to vasodilation. Direct vasodilator nerves that activate with the decreased sympathetic activity have been shown in multiple tissues, but their physiological significance is not evident [30, 31].

2.1.2 Disorders or Diseases Affecting the Microvasculature

Microvascular disorders or diseases can disrupt the functions of the microvasculature and provide insufficient nutrients to parts of the body. Acute disorders,

such as spinal cord injuries, can sever the connection between the vessels and the ANS, deregulating the two subsystem. More degenerative systems, such as type II diabetes Mellitus, slowly diminishes the endothelial and can ultimately lead to complications such as blindness [32].

2.1.2.1 Spinal Cord Injuries

Spinal cord injuries (SCI) can be considered the most devastating of all traumatic events, with around 15 to 52 cases per million of population per year. Of these cases, 80% are young males between 15 and 35, and 5% are children [33]. SCI implies degeneration in the descending pathways from the central system, impairing autonomic functions. The loss of control over the sympathetic system results in a decrease in sympathetic activities although parasympathetic tone is often preserved. The balance between the two opposing systems is interrupted and parasympathetic outflow becomes unregulated [34]. This has a detrimental effect on the cardiovascular system, and cardiovascular events are thus the leading cause of death in both initial and chronic stages of SCI [35]. Microcirculation suffers greatly with the inhibition of the sympathetic control, potentially leading to diseases such as hypoxia and ischemia [36].

Autonomic dysreflexia (AD) is a common complication of individuals who undergo SCI, especially patients who experience the injury at level T6 or above. An episode of AD involves a large increase in blood pressure and bradycardia and can be life-threatening. Typically, the onset of an AD episode is due to irritation of the urinary bladder or colon. An event triggers a massive sympathetic discharge at or below the location of the SCI, inducing major vasoconstriction and increasing BP [37]. Baroreceptors above the

injury location sense the raise in blood pressure and active the parasympathetic nervous system. Due to the injury, sympathetic inhibitory signals are blocked from being transmitted below. As a result, parasympathetic nerves control above the injury and sympathetic nerves prevail below with the uncontrolled sympathetic tone dominating, and thus increasing BP [38].

Assessment of a patient after a SCI can help facilitate improvement for both the acute and chronic phases. However, there is no single definition of completeness of injury. Many professionals just classify the injury as "complete" or "incomplete," where "complete" just represents a lack of axons crossing the injury sights. However, it is suggested that a person can recover some functions when the spinal cord is re-perfused or decompresses. The American Spinal Injury Association (ASIA) attempted to further classify completeness with and A-E scale with A being complete and E being normal [39]. This classification relies heavily on sensory and motor function and does not account for autonomic control. A method to analyze the autonomic control of a patient would help classification along with treatment.

2.1.2.2 Type II Diabetes Mellitus

Type 2 diabetes mellitus is a global health issue effecting approximately 180 million people worldwide, 95% of all diabetics. The number of people affected is predicted to double by 2030 [40]. Type 2 diabetes is defined by high glucose level (hyperglycaemia), insulin resistance, and lack of insulin [41]. The disease is associated with wide arrange of microvascular disorders such as retinopathy, neuropathy, peripheral vascular disease and cerebrovascular disease. With the degenerative nature of the disease, early state diabetics

will have little to no microvascular complications while later states will exhibit several [40].

Endothelial dysfunction is a common finding with patients with diabetes. When endothelial cells are exposed to hyperglycaemia, they undergo an apoptic process (leading to the death of the cell) and detach from the vessel. Without the endothelial reconstruction, undesired processes could be triggered, such as smooth muscle growth, migration and matrix secretion. However, hyperglycaemia also targets endothelial cell precursors (ECPs), or immature cell capable of transitioning to mature endothelial cells. Diabetics not only have less ECPs circulating though the body, but the ones that do exist have less functional capabilities including reduced adhesion, migration and proliferation [42]. Being able to monitor diabetes at an in-home system could help identify early signs of degeneration or track the progress of certain drugs or treatments [32].

2.1.3 Current Microvasculature Assessment Techniques

2.1.3.1 Catheter Angiography

An angiogram is a common technique for assessing microvascular health in specific regions of the body. A special dye called a contrast agent is injected into the blood stream and an imaging technique, commonly fluoroscopy, computed tomography, or magnetic resonance imaging, takes pictures of the region to be analysed by specialist. The angiogram is effective at revealing aneurysms, narrowing or blocking of blood vessels, and the presence of artery diseases [43].

Figure 5 – Using a fluoroscopy, an angiogram is able to take images of the microvasculature with the injection of a contrast agent. Image used under GNU free Documentation License [1]

An angiogram utilizing a fluoroscopy typically takes between one to three hours. Usually, an IV is inserted into the patient, and an area chosen by the doctor is shaved and cleaned. Local anaesthetic is applied to numb the region. A needle attached with a guide wire is inserted in either the femoral or brachial artery. Using the fluoroscopy as feedback, the specialist navigates the guide wire to the area of interest. A catheter – a small, flexible hollow tube to deliver the contrast agent – is then placed over the guild wire to the blood vessel. The dye is injected through the catheter and the fluoroscope takes pictures and records the resulting images [43].

Administrating an angiogram to continuously monitor a patient's microvascular health is difficult due to the amount of risk involved in the procedure, the personnel required, and the expensive equipment needed. Thus – although the angiogram is used for

initially diagnosing microvascular dysfunction – it is not a tool that can be used for longitudinal monitoring.

2.1.3.2 Flow-Mediated Vasodilation

Because it is a non-invasive technique, flow-mediated vasodilation (FMD) has become one of the most common approaches to assess endothelial function (and, accordingly, microvascular health) [11]. The method induces reactive hyperaemia, or a local increase in blood flow, by temporarily occluding and then suddenly releasing pressure around a peripheral artery. The increase in flow causes an increase in shear stress. As stated earlier in this work, shear stress causes a chain of reactions to eventually stimulate the generation of NO to the smooth muscle, causing vasodilation that can quantified. Though widely used due to its non-invasive nature, FMD does have certain limitations [44].

FMD typically takes place in a clinic with the room at room temperature and the subject close to homeostasis. The subject is positioned in a supine positon with an arm in a comfortable position. A sphygmomanometric cuff is placed either above the antecubital fossa or on the forearm. An ultrasound system with software to capture two-dimensional imaging, color and spectral Doppler, and a high-frequency vascular transducer is positioned above the brachial artery. Images are taken to act as the baseline. Pressure in the cuff is inflated well above systolic pressure to ensure complete occlusion of the area and downstream arteries dilate due to autoregulatory mechanisms. After a set length of time, the cuff is deflated, and due to the downstream dilation, a period of high-flow occurs through the brachial artery, increasing shear stress and dilating the artery. The ultrasound continuously records the artery from 30 seconds before deflation to 2 minutes after [45].

Figure 6 – Image of flow mediated dilation procedure. The cuff is inflated, creating a reactive hyperemia downstream. As the cuff is removed, the reactance of the brachial artery is monitored with an ultrasound. In [3], used with permission.

While analyzing the variability of the post-stimulus arterial diameter is an effective way to assess endothelial function, FMD includes many of the same limitations as catheter angiography due to its bulkiness and the cost of the procedure. A trained professional who can administer the test and translate the response is required. The angle with which the ultrasound probe is held over the arm can affect the accuracy of the results. The procedure is uncomfortable for the patient, as the cuff occludes the artery for several minutes. In addition, while the reactivity of the brachial artery has been shown to increase with drugs known to reduce cardiovascular risks, it is unclear how an improvement in the reactivity translates to an improved outcome [45].

2.2 Proposed Modulation Approach: Temperature Stimulus

The assessment of microvascular health fundamentally hinges on testing the ability of the vessels to *react* to some form of external or internal stimulus. Ideally, a known and quantifiable stimulus should be applied, and then a quantifiable set of objective parameters describing the physiological response should be measured and assessed. Several non-invasive methods are available to modulate vascular tone including thermal stimuli, various breathing exercises, evoking mental stress, and transdermal delivery of vasoactive components [46]. Our approach focuses on modulating *skin temperature* to induce a response in microvascular tone. This method is safe, easy to implement, and is well studied in the lab. Additionally, thermal stimuli can result in both local (endothelium and VSM) and central (ANS) responses.

Humans rely on thermoregulation to maintain a constant core temperature even in the presence of thermal stress. Multiple factors can create thermal stress, such as external temperature or heat produced internally during skeletal muscle activation. The body responds to such stresses physiologically with changes in heat dissipation or heat generation by modulating vascular tone, sweating, or shivering. In a healthy individual, the body will respond to cold with heat conservation through vasoconstriction or to heat with heat dissipation through vasodilation. The central mechanism that acts as the thermostat for the body is the preoptic/anterior hypothalamus. Information pertaining the core and skin temperature is relayed to the hypothalamus which sends the appropriate signals to induce the appropriate response. In this manner, this system essentially acts as a negative feedback loop to regulate body temperature. The response of the system will change proportionally with temperature until either body temperature is stable and heat dissipation and heat generation are equal or a maximum response is reached [13].

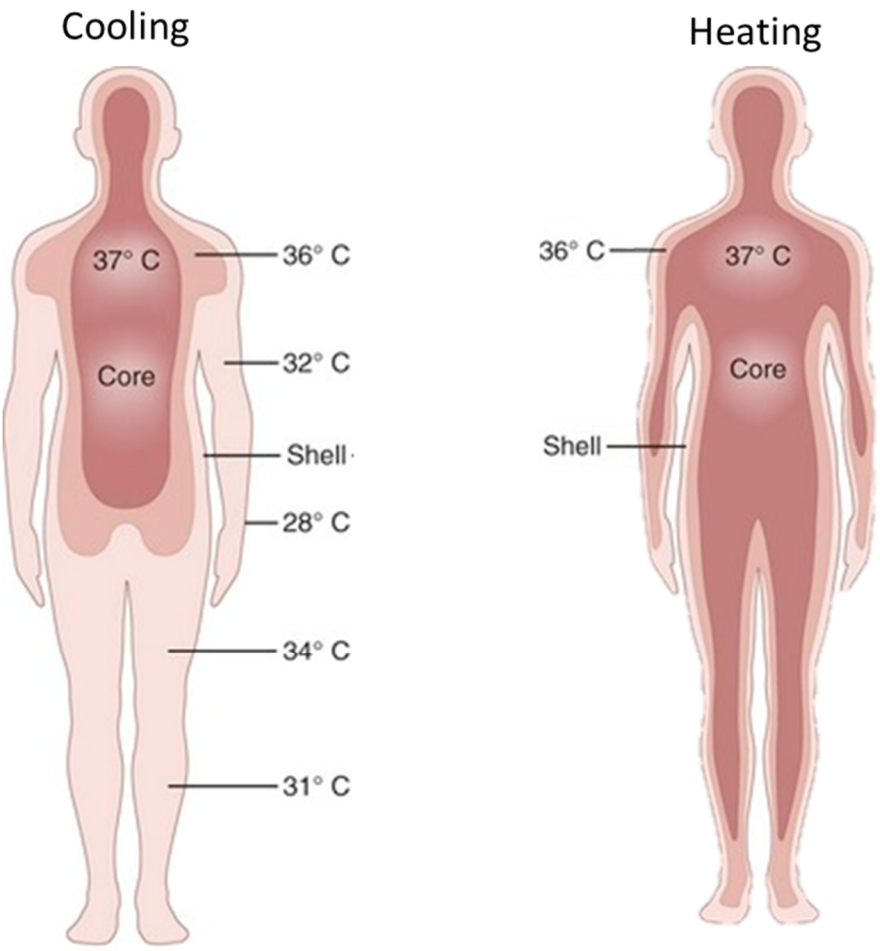

Figure 7 – Image showing the response to thermoregulation during both full body cooling and heating. During cooling, blood flow is restricted to the peripherals to conserve heat to vital organs. Heating has the opposite effect, skin blood flow increase, removing heat from the body.

A major influence in the control of body temperature is skin blood flow. Modulation of skin blood flow can have a great effect in managing heat stress. In normal conditions, cutaneous or skin blood flow can average around 5% of cardiac output [23] which translates to approximately 80 to 90 kcal/h of heat dissipation, similar to the level of resting metabolic heat production [47]. During extreme cold stress, the cutaneous blood flow can essentially become zero, while at high levels of heat, the blood flow to the skin can reach

7 l/min, which is approximately 1.5 – 1.75 times the normal resting cardiac output of a healthy person at rest [2].

The type of skin – non-hairy (glabrous) or hairy (non-glabrous) – will affect the response to temperature stimulation. Glabrous skin covers areas of the body near specialized organs or structures such as the palm and forehead and acts as a radiator for the organs. Common features exhibited by this type of skin include absence of hair, dense vascularization, and large surface-area-to-volume ratio [48]. A major contributor to the increase in heat dissipation in glabrous skin is the abundance of arteriovenous anastomoses (AVA). AVAs are a direct connection between small arterioles and small vein. They contain no capillary segments and their only function is to transport heat from the core of the body to the skin [49]. Many of these organs and structures are located distally and require an effective control of heat. These radiators have the ability to dramatically increase blood flow to rapidly expel heat. For example, the glabrous skin on the human finger is able to increase flow by fivefold. AVAs are also able to slow down blood flow to essentially zero to minimize heat loss. This method is usually the body's first line of defense in thermoregulation since glabrous skin does not require either water or energy for vasodilation or vasoconstriction**.** Non-glabrous skin is characterized by the presence of hair follicles and the lack of AVAs. As opposed to glabrous skin acting as a radiator, non-glabrous skin acts more like an insulator and the temperature is more stable. Typically, these areas exist more peripherally than non-glabrous skin and cover approximately 95% of the body [48].

Independent of skin type, all skin areas are controlled by both neural control and local control mechanisms. On the neural side, the skin areas are supplied with sympathetic

vasoconstrictor fibers attached to the vascular smooth muscle whose responsibility is to modulate norepinephrine from their nerve endings for vasoconstriction and vasodilation. During normal conditions, tone is maintained through nerve discharges occurring 1-3 times per second with the discharge rated affecting the vascular tone. Non-glabrous skin areas also have active vasodilatory nerve fibers, also stemming from sympathetic origins. The roles of these nerves are less clear than the vasoconstrictor fibers, but it is speculated that the main neurotransmitter is acetylcholine to have a relaxation effect on VSM [50]. At a local level, the endothelium plays an important role in modulating skin blood flow during thermoregulation by regulating the release of nitric oxide in the vessel to either constrict or dilate the surrounding VSM.

2.2.1 Response to Heating

The response to heating varies dramatically with applied temperatures to the skin. Between 20 and 35 °C, the changes are relatively small. At temperatures above 37 °C, changes are much more dramatic with maximum effects occurring at 42 °C. When the maximum temperature is applied rapidly to the skin, skin blood flow over a short period of time increases to its maximum level. At this temperature, VSM is fully relaxed and therefore unaffected by subtle changes in vasomotor activities that exist in other levels of vasodilation. This response is typically used as a baseline when measuring blood flow or vascular conductance, allowing for comparison between subjects or between different sites [2].

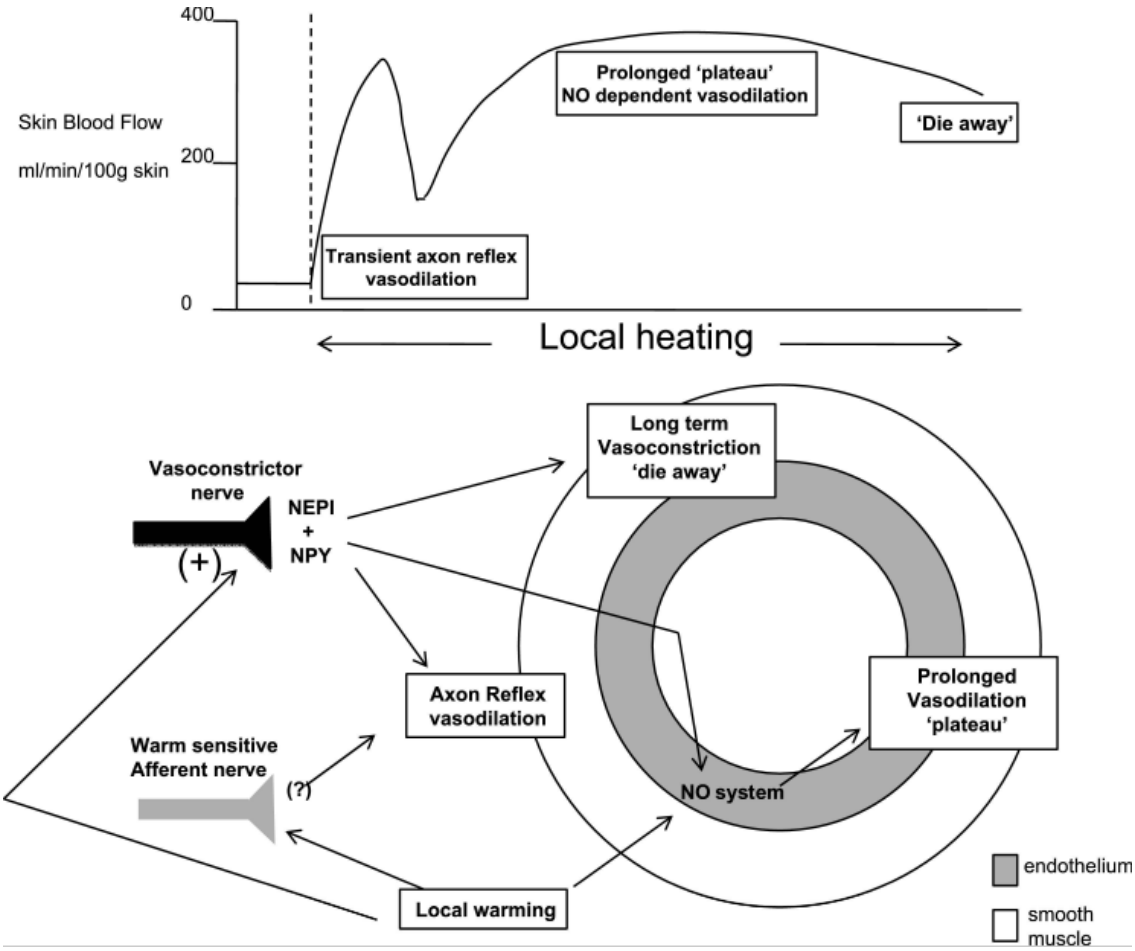

Figure 8 – The response of both the sympathetic and sensory nerves during local heating of blood vessels. From [2], used with permission

As the skin reaches its maximum blood flow with applied heat, the skin blood flow actually undergoes both vasodilation and vasoconstriction. Within the first 3 to 5 minutes, blood flow increases rapidly to an initially peak, around 75% of maximum skin blood flow [51]. The dominating factor involved in this initial response relies primarily on the sensory nerves in smooth muscle, specifically heat-sensitive nociceptor. Vanilloid receptors on the nerve endings are partially responsible for transducing sensations [52]. After the initial increase in blood flow followed by the moderate decrease, skin blood flow slowly increases to its maximum. This phase is greatly influenced by nitric oxide, both initiating and

maintaining the phase and forming a plateau-like response [13]. Upon heating of the skin for 40 minutes, skin blood flow reached a near maximum value [51].

Sympathetic vasoconstrictor nerves are required for both the initial peak caused by the sensory nerves and the release of NO in the endothelium for vasodilation. Though this sound counterintuitive that vasoconstrictor nerves would cause vasodilation, it has been shown that these adrenergic nerve transmitters bind to α_{2-} and Y_1 receptors on endothelial cells, releasing neurotransmitters norepinephrine and/or neuropeptide Y and stimulate NO synthase [53].

In regards to whole body effects, heat stress has a direct effect on many cardiac functions. Cardiac output during heat stress increases and can increase well above 10 L / minute with whole body heating. Stroke volume is relatively constant, thus heart rate increase serves as the driving force behind the increase of cardiac output [14]. The baroreflexes are partially responsible for the increase of cardiac output, allowing blood pressure to decrease minimally (3-5 mmHg) even with the substantial vasodilation and increase in arterial compliance [54]. In addition, baroreflex regulation of the heart leads to a decrease in the high frequency aspect of heart rate variability, an index of cardiac sympathetic activity [55].

2.2.2 Response to Cooling

As previously mentioned, local cooling of the skin can cause vasoconstriction, decreasing the skin blood flow and conserving heat in the body. With enough heat removed from the skin, blood flow can essentially go to zero to reduce, to the extent possible, any excess heat loss. Vasoconstriction is due to primarily to three mechanism: the inhibition of

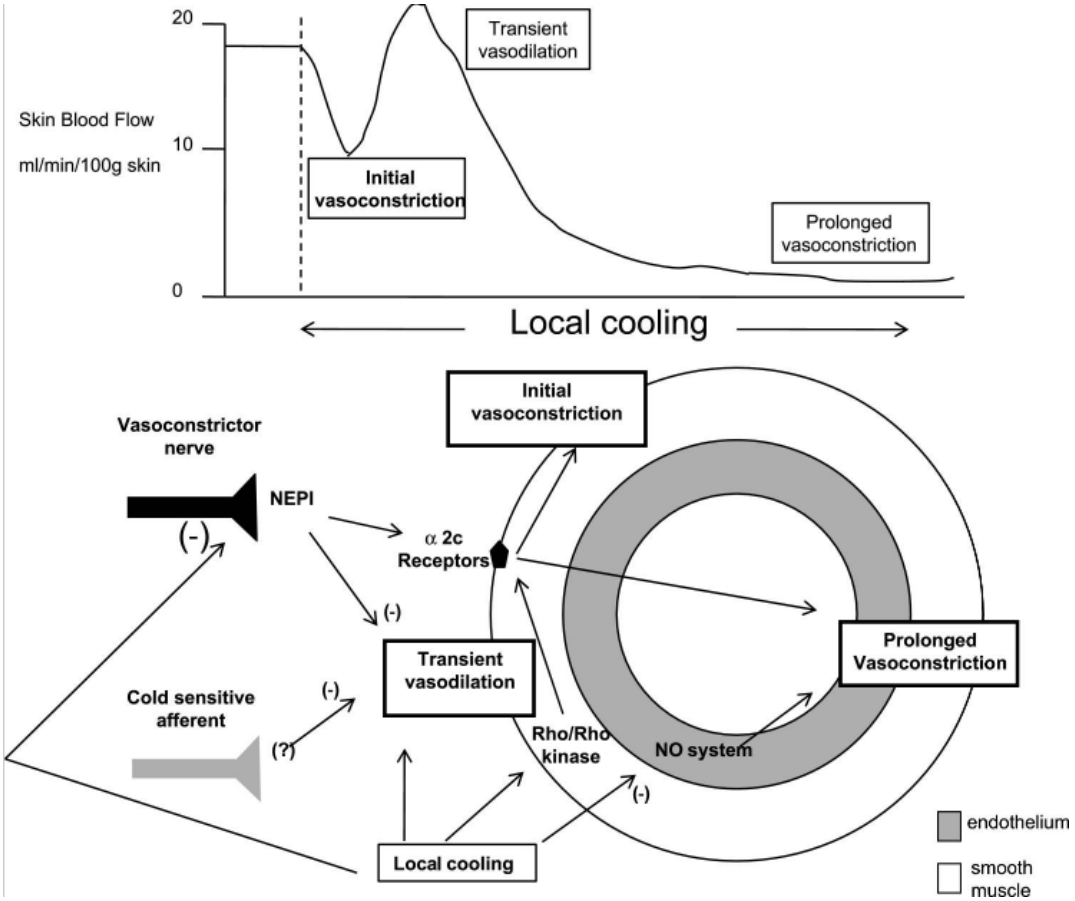

Figure 9 – The response of both the sympathetic and sensory nerves during local cooling of blood vessels. From [2], used with permission.

the NO system at multiple points, the involvement of postsynaptic upregulation of a_2 receptors and the activation of cold-sensitive afferents [2].

As with heating, the first response is due in part to sensory nerves. The perception of cold temperatures can be felt when the skin is cooled down by 1 °C. The response of calcium channels begin at around 28 °C, with an increase in activity as the temperature decreases and saturates at around 10 °C [56]. The activation of the calcium channel is believed to cause a release of neurotransmitters, in particular norepinephrine, for vasoconstriction [57].

With the continuation of applied cooling, the vasoconstriction mechanisms are halted and the vessels undergo cold-induced vasodilation (CIVD). When a person is initially exposed to a cold source, heat production is dramatically increased through sources such as metabolic rate and shivering. Heat production increases past the rate of heat dissipation, overshooting body temperature. It is speculated that CIVD is a response to this overshoot [58]. As cooling continues, vasoconstriction occurs continues due in part to the inhibition of the nitric oxide system [59]. Vasoconstriction has also been seen at sites downstream of local cooling. This was indicated when a NO donor was applied to the affected region and vasoconstriction was still observed [60].

Adrenergic functions are another main component in cool induced vasoconstriction. Local cooling primarily alters the postsynaptic receptors, stimulating the mobilization of α_2 –receptors [2]. This receptors are redistributed on the VSM cell with the cold-inducted activation of Rho kinases, allowing for a more efficient response to norepinephrine. With the initiation of a more central mechanism, sympathetic adrenergic nerves increase the release of neurotransmitters and cotransmitters [61]. These responses work in collaboratively to induce vasoconstriction

With regards to heart rate, the effects of local cooling are not well defined. Both increases and decrease in heart rate have been observed during cold pressor studies [16]. Since stroke volume generally remains constant during cold exposure, cardiac output varies based on these changes in heart rate. Even though there are inconsistencies with cardiac output, blood pressure generally increases [62]. The increase in vascular resistance associated with vasoconstriction can cause blood pressure to increase by approximately 13 mmHg during a cold pressor test [63].

2.3 Instrumentation Background

In our proposed setup, two systems in particular will need to be understood in order to modulate skin temperature and then measure the responses: thermal electric coolers (TECs) for modulating temperature and photoplethysmography (PPG) for measuring the physiological response. Temperature modulation causes variations in heart rate and blood flow, parameters that can be monitored to some extent with a PPG sensor. TEC components utilize the Peltier effect to create a temperature gradient across two sides and can both heat and cool the skin, allowing for modulation in both directions.

2.3.1 Thermal Electric Coolers

Thermal Electric Coolers are used in the system to either cool or heat the skin. These components utilize the Peltier effect to create a temperature gradient across two sides. The effect occurs when a current flows through two different junctions of conductor-semiconductor [64].

While the efficiency of TECs is far below alternative heat pumps, TECs advantages outweigh the disadvantages. Unlike traditional heat pump, there are no moving parts. To

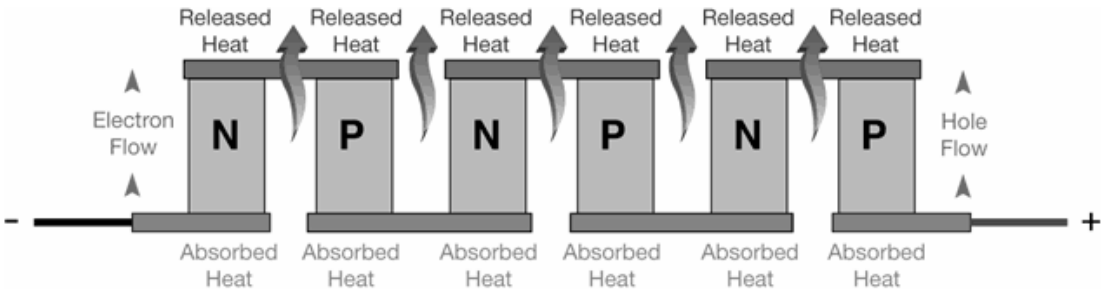

Figure 10 – Image showing the transfer of heat with an applied voltage. Image Used under Creative Commons Attribute License.

change the temperature, only an electrical current is required. In addition, the TECs is able to transition from heat to cold just by changing the direction of the current. This will allow for multiple modes of operation without adding extra component. Finally, TECs are low profile compared to standard heat pump, allowing direct integration in many applications.

2.3.2 Photoplethysmography

Photoplethysmography is a common measurement for oxygen saturation, heart rate, and blood volume changes. PPG is measured using a light source and a photodetector (photodiode, phototransistor, etc.). Emitted light penetrates through the biological tissue and is absorbed by skin, bones, and arterial and venous blood, then detected on the other side of the tissue (for the most common transmissive mode of PPG). During systole, more blood enters the measured area and the diameter of the arteries increase, thus increasing the attenuation of the light passing through the tissue. Therefore, two components are measured, a DC value associated with non-pulsatile components and an AC value corresponding to the pulsation of the arterial blood [65]. The DC component will vary slowly based on respiration, vasomotor activity, and thermoregulation, but will typically fluctuate at frequencies less than 1 Hz [66].

CHAPTER 3. INSTRUMENTATION DESIGN

To induce responses in the microvasculature to controlled stimuli, local heating and cooling was applied to the skin of the hand. As a preliminary study, heat packs and cooling packs were interchanged during the studies [67]; however, this led to inconclusive results. While physiological changes were noticed, they were inconsistent between subjects. Both packs were unable to sustain a constant temperature profile throughout the testing protocol. While this method has the possibility of inducing an initial response to heating/cooling, the effect was short in duration. The thermal capacity of the heat/cold packs was not sufficient to counter the body's ability to sink or source heat. In addition, the packs needed to be placed and taken off the subject's hand during the experiment. This changed the applied pressure to the subject's hand, which has the potential to further skew the results. In addition, the repeatability of the test was low due inconsistencies in the procedure such as the initial temperature of the packs. An improved system utilizing TECs was developed to maintain a constant skin temperature profile by continuously sourcing or sinking heat from the hand to either heat or cool, respectfully.

3.1 Physiological Measurement Techniques

The proposed system relies on applying an active thermal stimulus to a person's hand, and monitoring the physiological responses using three common biosensing techniques: PPG, BP, and ECG. Each sensing technique can be adapted to allow for inexpensive integration into a final device that could be deployed in a subject's home.

The PPG signal was measured using commercially available devices extensively used in clinics. The implementation of this system into the glove hardware will be discussed in a later section below. BP was monitored with the use of the ccNexfin (Edwards Lifesciences, Irving, CA), operating based on the volume-clamping method [68]. Note that while this system is not feasible for an at-home system due to the high price and inconvenience, an alternative BP measurement approach, such as one based on pulse transit time, could be used instead in future systems [69]. The ECG was recorded using commercially available devices from Biopac Systems (Goleta, CA).

3.2 Glove Design

A glove-based system was selected for the following reasons: the orientation of the device onto the body is well-controlled, the glove fully encapsulates an area of the body for tight thermal control, and the hand is a site on the body that is well-perfused. A polyester athletic glove (UA ColdGear Infrared Engage, Under Armor, Baltimore, MD) was initially used both to house the electrical components and to provide a layer of thermal insulation. The elastic nature of the glove ensured a tight fit to the hand and proper contact pressure between the skin and TECs to increase thermal conductivity. Thermal insulation tape was placed in the inner lining of the glove to further insulate the glove.

TECs known as Peltier tiles were used to modulate the temperature of the glove. Six CP85338 (CUI Inc, Tualatin, OR) Peltier tiles were selected. Each one of these 30mm x 30mm tiles has a max 14.5V and 2.5A rating to achieve the maximum ΔT. At room temperature (25° C), the maximum heat absorbed at 0 ΔT is 21.4W and maximum

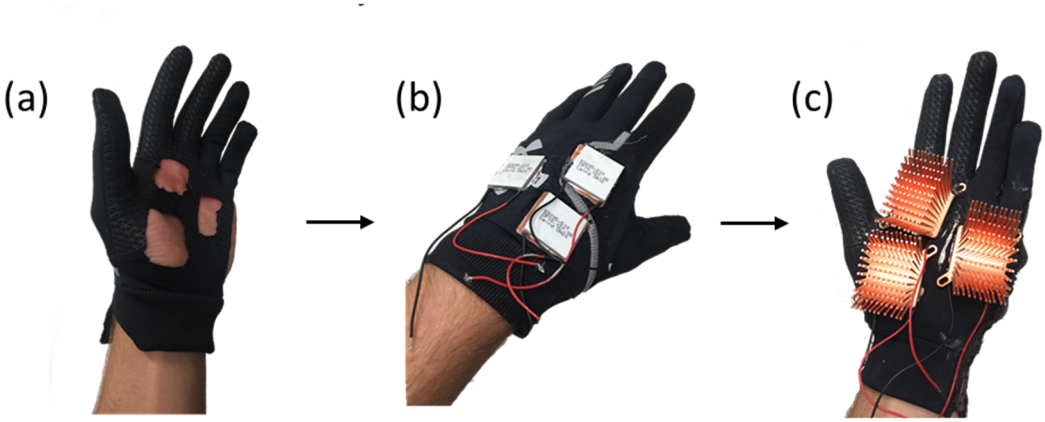

Figure 11 – Flow diagram of the gloves progression during construction. Square slots were cut out to insert copper plates and Peltier tiles. Copper heat sinks were placed on top to remove excess heat from the tiles.

temperature gradient is 68 °C when Q is 0 (when the maximum amount of heat is transitioned from one plate to the other). With 21.4 W per tile, the glove will initially be able to transfer a total of 128.4 W, which will provide more than sufficient heat and cooling to stimulate a vasomotor and neurovascular response.

Copper foil was placed in the inside of the glove and six squares of the glove were removed to reveal the copper. The copper served a dual purpose: to attach the TECs to the glove and to help evenly disperse the heat to the skin. The TECs were attached on top of the copper foil using thermally conductive epoxy. A copper heatsink was attached to the top of the Peltier tiles to remove any excess heat (CNB-S1, Enxotech Northbridge, Kirkland, WA), again using the thermally conductive epoxy. Since it is important to sink away the heat from the inefficient Peltier tiles, copper, with its high thermal conductivity, was chosen as the material for the heat sink (385 W/m K compared to Aluminum's 205 W/m K). Finally, a fan was attached to the heatsinks to further remove the heat and to prevent overheating.

3.3 Temperature Modulation Techniques and Characterization

Controlling the TECs is required to achieve a consistent temperature profile throughout the testing. Typically, such high-current (many Amps) applications employ either pulse wave modulation (PWM) or a DC voltage. PWM provides a simple and flexible means of varying output power; however, PWM control can become problematic when used with TECs. With the increasing duty cycle, the root-mean square (RMS) current increases, and thus substantially more heat is generated through ohmic losses in the tiles [70]. Faster transients can also create thermal stress on the device, shortening the device's lifespan [71].

To provide the variable voltage while being able to maintain the high current flow, the OKR-T/10-W12 10-Amp DC-DC converter was used (Murata Power Solutions). A power output of 50 W will suffice to safely power two Peltier Devices at once. A total of 3 converters were used to power the six tiles. On/off pins on the converters were used to set the output voltage to 0V to allow for baseline room-temperature measurements or during emergency shutoff. A pin was available to attach a trim resistor capable of setting the output voltage between 0.591V and 6V. The resistor value was calculated using the following formula:

$$R_{Trim}(k\Omega) = \frac{1.182}{V_{out} - 0.591} \tag{4}$$

Ideally, a continuous potentiometer would allow for an infinite set of possible V_{out} values, though the relationship is nonlinear. However, to control the potentiometer with this digital

signal from a microcontroller, a digital potentiometer was placed as the trim resistor. These resistance elements contained a "wiper" that varied between a finite number of positions or "taps." To cover the full range of values, a 5kΩ 64-tap digital potentiometer was used (MCP4011, Microchip Technology, Chandler, AZ). While this resistance value provided the advantage of covering the full range of values, considerable voltage steps occurred at the lower resistance values. At 218Ω the output voltage of the DC-DC converter was 6V. By varying the wiper just one position, the resistance of the trim resistor became 297Ω and the output voltage became ≈4.6V. While this can cause ripple in the Peltier tiles, the ability to use the full range of voltage values was deemed a higher priority for the initial prototype. Longer protocols will require an exact control of voltage to minimize overheating.

The outputs of the DC-DC converters were attached to the input of two single pole double throw (BR010134, ITEAD studio, Shenzhen, China). A single digital input controlled the wiper for both relays. Each common node of the relays is attached to one end of a Peltier tile. The voltage output of the DC-DC converter is placed on one of the varying pins for both relay in such a way that the voltage output was connected to only one input of the Peltier device at a certain state. The ground pin of the converter was connected to the two remaining pins of the relays. The configuration allows the bias and therefore the current to be reversed when the relays are active and the switch is thrown. Figure 13 shows a diagram of this setup.

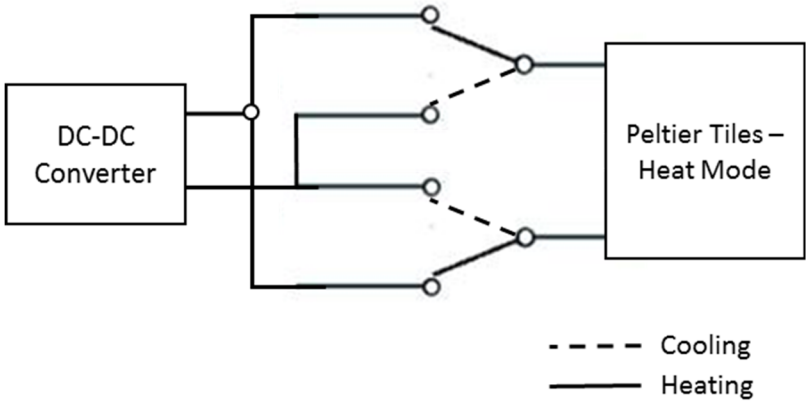

Figure 12 – A set of single pole double thrown configured to act as an H-bridge, allowing for bidirectional current flow.

Measurement of temperature during testing is required to provide feedback to the microcontroller to allow for precise temperature control. A thermistor chosen to read the temperature from the glove is the 252FG1J (US Sensor, Orange, CA). This thermistor is small enough to fit inside the glove and to be placed between the skin and the Peltier tiles. A voltage divider was constructed with a 5.1 kΩ resistor with the output being sent to a microcontroller, allowing for a resistance calculation. The thermistor operates at a range of -55 °C to 300 °C, much greater than the range required for this application.

Assuming a linear voltage/current response from the TECs, a single tile will draw approximately 1.03 amps of current. With the six tiles running concurrently, the total current will exceed 6 amps. The ILG-500-2 500 Watt ATX Power Supply (Inland Products, Fullerton, CA) was connected to the DC-DC converter to supply the necessary power. The power supply contains both a +5V line and a +12 line, providing the necessary voltage for the microcontroller, the cooling fan, and the tile. The +12V connected to the DC-DC converter has a max current output of 28A, providing more than sufficient current to the tiles. If an increase in cooling/heating is required, the power supply could also supply the

15A of current to run the six tiles at their maximum output. Note that these high current values were used in the initial prototyping phase to ensure that the glove could achieve substantial modulation of skin temperature in short periods of time (i.e., > ±10 °C in < 1 min). In future work, it may be possible to operate at much lower temperature swings and over longer time intervals, in which case less operating current may be acceptable.

The Arduino Uno (Arduino LLC, Somerville, MA), was chosen as the microcontroller platform to communicate with the multiple components of this system, due to its ease of use and versatility. The Arduino is based on the ATmega328P, a picoPower 8-bit microcontroller developed by Atmel. The controller's specifications, seen in Table 1, are sufficient for this project. The analog input pins with 10-bit analog resolution acted as the analog to digital converters to read in the output of the thermistor's voltage divider. Digital outputs controlled the three sets of relays, switching between cooling and heating states. Two more digital outputs communicated with the three digital potentiometers simultaneously. A fourth digital output was attached to the "enable" pin of the power supply, allowing the system to turn off if a fault is detected. Finally, as the Arduino Uno supports serial peripheral interface (SPI) communication, a USB-A to USB-B line was connected between the Arduino and a laptop computer with SPI, sending 8-bit characters between the two units.

Table 1 – Arduino Specifications

Parameter	**Value**
V_{Supply}	5V
Digital I/O Pins	6
Analog Pins	6
Flash Memory	32 KB
Clock Speed	16 MHZ

3.4 High-Level User Interface

A Matlab (Mathworks, Natick, MA) graphical user interface (GUI) was developed to perform the high level controlling of all the systems. The front panel of the GUI can be seen in Figure 15. By pressing "Set Up Serial Port," the GUI initiates the communication with the Arduino through a COM port with the desired path being initialized in the text box below and is the first step in commencing a test. "Close serial port" properly disconnects the Arduino and should be utilized before disconnecting the Arduino or closing the GUI. The table in the lower left section sets the temperature gradient (ΔT) between the temperature at rest and the current glove temperature in the left column and the length of time in seconds to be held at that temperature in the right column. A positive non-zero entry will set the relay to the "heating" setting and a negative non-zero will set the relays to "cooling." The current temperature of the thermistors are shown in the top right, and the temperature at rest is shown directly below. This number is obtained from taking the average temperature of the first round of measurements. A "Start" push-button initializes the test. The push button changes to "Stop" when pressed, allowing the test to stop by the user at any time. Finally, the current state of the glove is shown below the push button along with the time remaining at that temperature gradient.

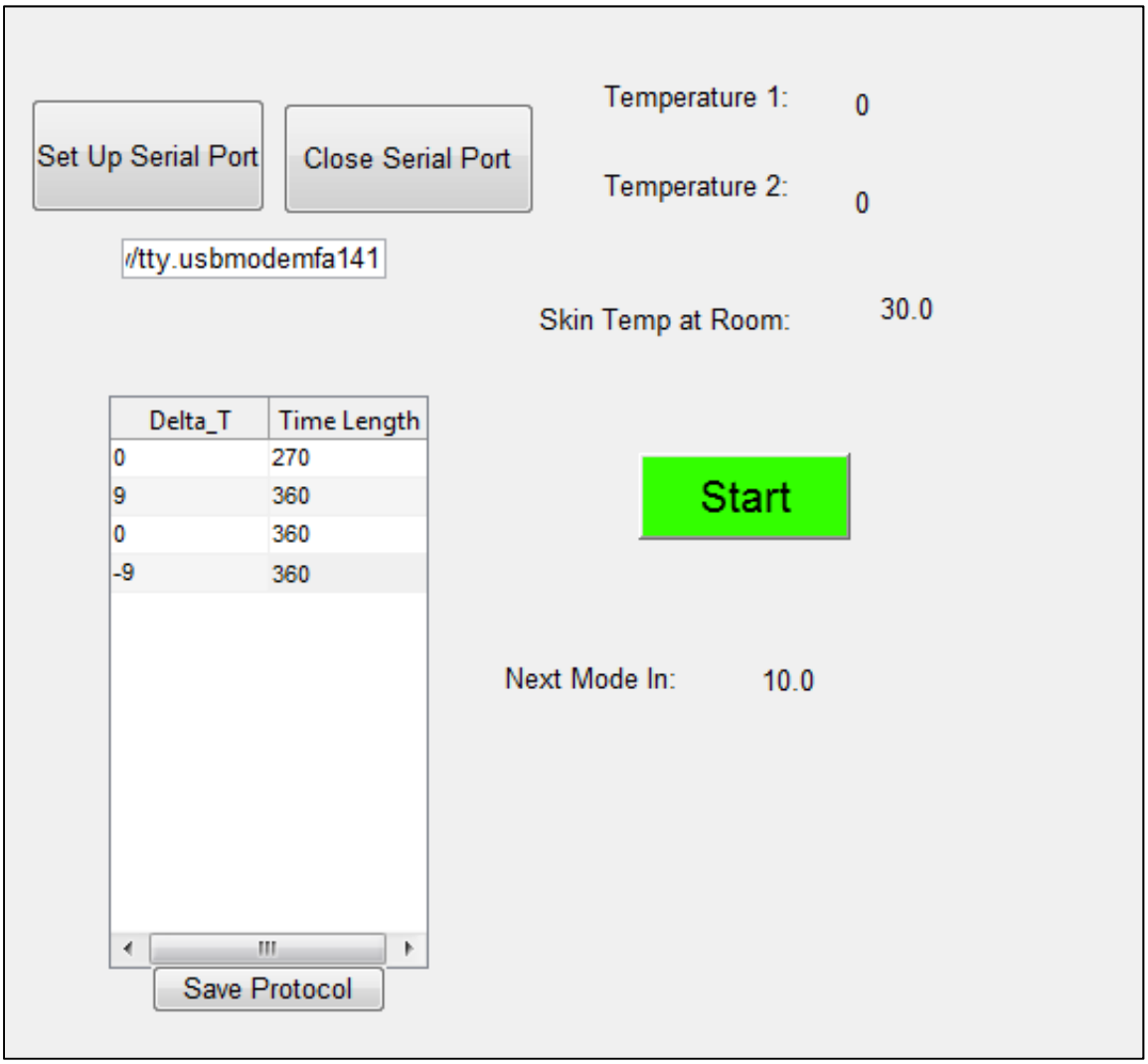

Figure 13 – Front panel of the Matlab graphical user interface (GUI).

After the user presses the "Start" push-button, the power supply turns on and the potentiometers are reset to the largest resistor value, reducing the voltage across the tiles to their minimum value. The code then starts cycling incrementally through the entered ΔTs. The code then implements a modified proportional-derivative (PD) loop to control the temperature based on the baseline temperature plus the current ΔT. Every tenth of a

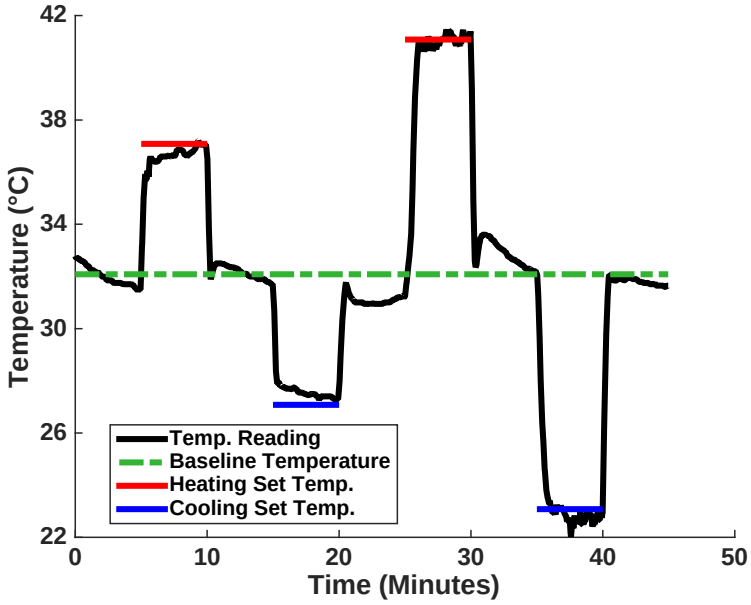

Figure 14 – Graph showing the temperature readings as the set point fluctuated from heating to cooling.

second, the temperatures of both potentiometers are read from the Arduino and averaged together to trigger the feedback, and an error value is calculated by subtracting the current value by the desired value. This error value (P) and its derivative (D) are individually gained and summed together. This value is then compared to the current value. If this error value is sufficiently large, the potentiometer will either increment or decrement, depending on whether the Peltier tiles need to further cool or heat the hand. The slow loop time constant and individual potentiometer incrementation was deliberate, reducing the thermal stress on the devices by eliminating quick and large fluctuations in current supplied to the tiles.

Due to the direct contact with the human body, safety was a major concern in the design. While not in use, the power supply was turned off to prevent any possibility of a

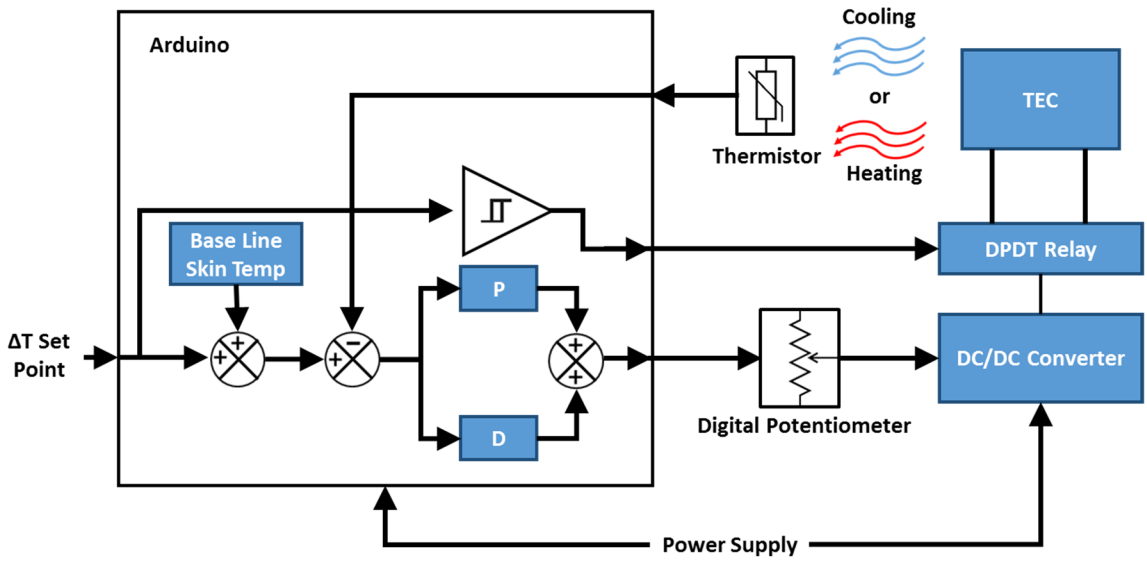

Figure 15 – Block diagram of the glove's control system. A change of temperature is set in the Arduino and is added to the baseline skin temperature. An error is calculated between the desired temperature and the measured temperature, and the present value and the derivative. (P/D) are used to determine the level of the resistor. This resistor sets the output voltage of the DC-DC converter, which is fed through a relay. Depending of the state of the relay, the TEC either warms or cools the hand and thermistor. The resistance of the thermistor is fed back into the loop and compared with the current temperature.

short in the system. While the test is running, if the user experiences any pain or discomfort, the "Stop" button can be pressed and the system will completely shut down. Due to the human body being more susceptible to pain at higher temperatures, the testing of the heating portion of the glove was especially rigorous. A max current limit was placed on the device setting a "safety-factor" far greater than that used for the cooling. In addition, the device automatically lowers the temperature if the temperature rises at too high of a rate.

Upon testing the device on multiple subjects, the average slew rate of the glove was found to be 0.13 °C per second during heating and -0.14 °C per second during cooling. The low slew rate ensures that the subject remains comfortable during the test and that pain-

induced sensor nerves are not activated during testing. This will maximize the probability that the reactions of the microvasculature are altered primarily through responses of the endothelium and autonomic nervous system. The accuracy of the system was calculated to be ±0.26 °C during heating and ±0.23 °C during cooling. The system was able to hold the inputted temperature value for the extent of the subject testing.

3.5 Physiological Sensing

For the ECG and BP measurements, standard commercially available products were used as described above. For the PPG sensing, custom circuitry was developed such that ultimately both transmissive and reflective PPG signals could be obtained from various positions on the hand integrated into the glove. The description of the circuitry used for PPG sensing is provided below.

A Nonin 8000SL finger pulse oximetry sensor (Nonin Medical Inc, Plymouth, MN) containing both a photodiode and a red LED working in transmissive mode was used for the sensing. The LED was powered with 16 mA of DC current. The photodiode was reverse-biased (5V) and input to the circuit shown in Figure 18.

The PPG analog front end consisted of three stages. The first stage is a transimpedance amplifier, converting the current output of the photodiode to a voltage signal. A low pass filter in the negative feedback of the transimpedance amplifier acts a first order high pass filter with a cutoff at 0.16 Hz. The 150kΩ sets the gain of this stage at 103 dB. A first order (RC) high-pass filter is then placed in series with a cutoff frequency of 0.3 Hz. An inverting amplifier with a gain of 46 dB and a first order low pass filter with a cutoff of 32 Hz is placed as the second stage. The final two stages are two cascaded

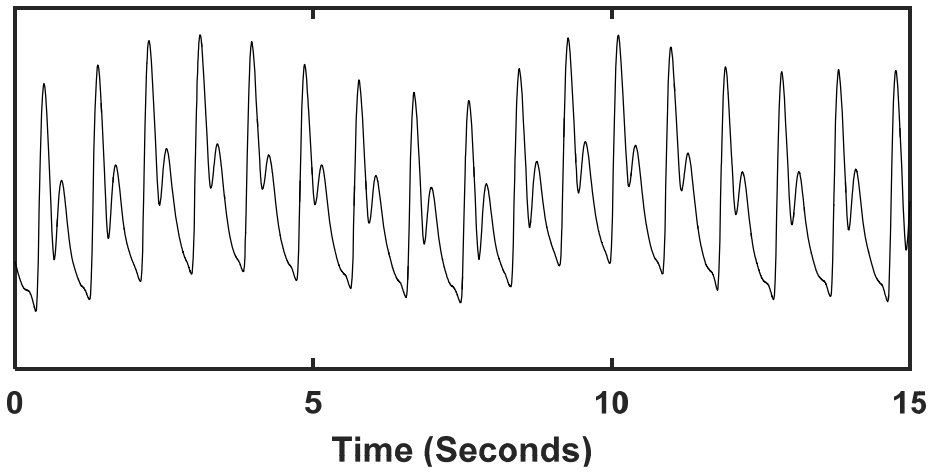

Figure 16 – PPG measurements from a subject's index finger. The higher frequency pulsation is due to the changes in blood volume during the cardiac cycle while the lower frequency variation is contributed to respiratory effects.

second order filters (Sallen-Key) with cutoff frequencies of 30 Hz and 20 dB each of gain. The op amp chosen for this circuit is the LT1678 due to its low input bias current and low voltage noise.

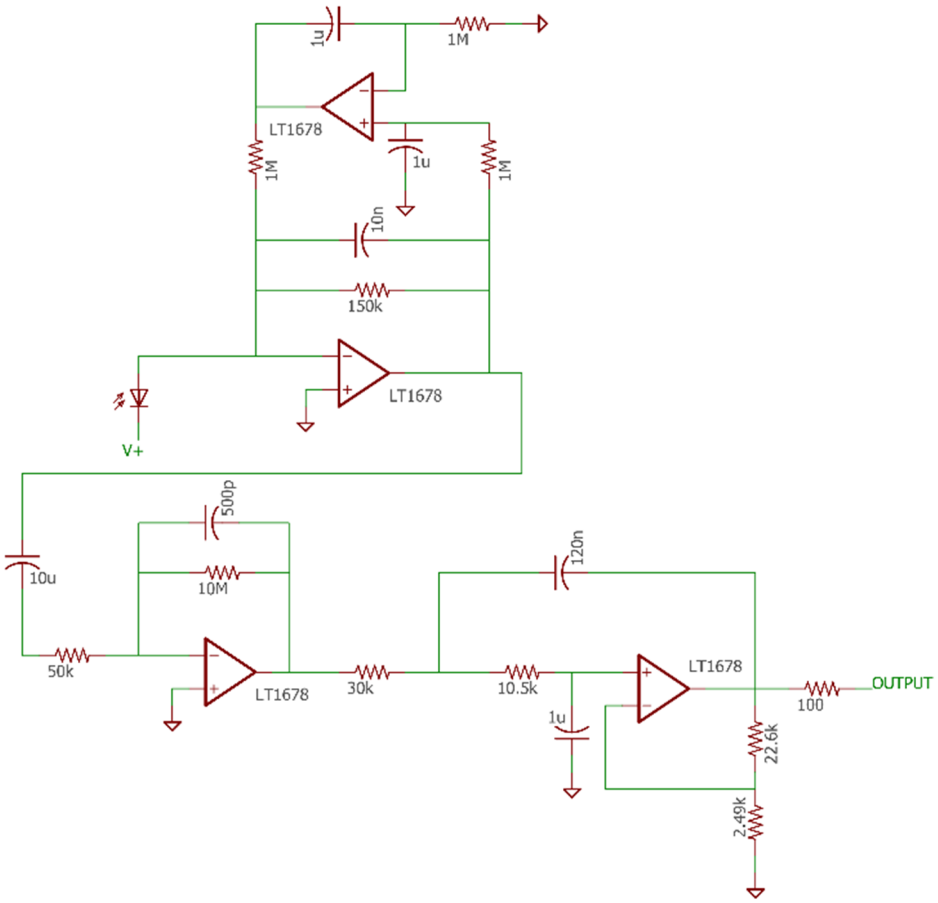

Figure 17 – Circuit diagram for the PPG front-end circuit. The three stages convert the output current of the photodiode into a voltage signal with an overall gain of 143 dB and a passband of 0.3Hz to 30Hz.

CHAPTER 4. METHODS

4.1 Testing Protocol

The human subjects studies were approved by the Georgia Institute of Technology Institutional Review Board, and all subjects provided written informed consent before participating. Six subjects were recruited to partake in the study (4 male and 2 female, Age: 23±2 years). The purpose of this study was to validate the glove's effectiveness in producing a repeatable physiological response. ECG, both finger PPGs, and BP were continuously monitored during the study. These signals were interfaced to a computer through a data acquisition unit and its corresponding software (MP150/AcqKnowledge, Biopac System, Goleta, CA). The data were sampled at a frequency of 2 kHz and stored on a desktop computer. The subjects were seated in a quiet temperature-controlled room and were asked to relax and remain still for the entirety of the study. During this time, there were no external visual or audio stimuli to unintentionally excite a neurological response and potentially confound the results. The glove was placed on the subject's hand, and the subject rested for four minutes before any testing began. This resting period served two purposes: (1) ensuring that the subject reaches further hemodynamic stability before the tests begin, and (2) allowing the glove's software to average the temperature to establish a baseline. The glove then transitioned to a heating phase where the temperature rose to 9º C above the baseline temperature for 3 minutes. After a quick cooling phase to transition the temperature back to the baseline and then three minutes of no temperature modulation, the glove cooled the hand 9º C below the baseline. This again lasted three minutes, followed

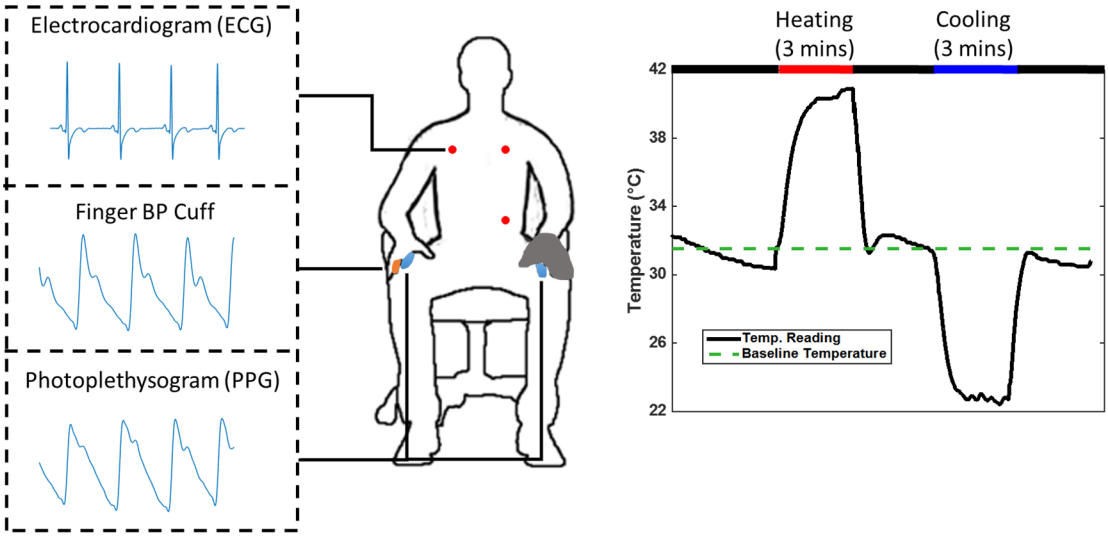

Figure 18 – Image of the experimental setup. ECG, a finger BP cuff, and two PPG signals record biosignals as the glove transitions from room temperature, heating, and cooling.

by a quick heating phase to raise the temperature back to baseline. Finally, the glove heated back up to room temperature and the subject rested for another 3 minutes.

4.2 Signal Processing

Much of the signal processing was completed using Matlab. The first step was to determine the locations of the R wave peaks of the ECG. This reliable point represented the start of the cardiac cycle. The ECG was first pre-processed with a Kaiser Window 0.5 to 40 Hz finite impulse response (FIR) filter. The peak timings were then found by taking the derivative of the sign of the first derivative of the ECG. Negative non-zero values represented positive peaks in the signal. A threshold of 1V was used to extract the R peaks.

PPG measurements were pre-processed with a Kaiser Window 0.4 to 8 Hz FIR filter. The BP measurement was left unfiltered due to linear filtering already being conducted in the ccNexfin device. Using the beats found by the ECG to locate the beats in the PPG signals, an ensemble average was found by taking the average of eleven PPG beats

surrounding the beat of interest (five before, five after). The purpose of the ensemble averaging was to eliminate any zero-mean noise uncorrelated to the heartbeats. The minimum and maximum of each beat were found to calculate the amplitude of the signal. The average amplitude was calculated for each bin. BP was determined simply by considering the average reading for each bin from the ccNexfin. A similar process was used to process the BP measurements. The maximum of the ensemble average represented the systolic blood pressure (SBP) and the minimum represented the diastolic blood pressure (DBP).

To calculate HRV, the difference in the R-peak timings were taken to determine the R-R interval. Using this method, the R-R interval was mapped out to the corresponding R-peak timing, resulting in a non-constant interval between samples; unfortunately, this non-constant sampling between successive points needed to be addressed to facilitate subsequent Fast Fourier Transform (FFT) computation. Interpolation of the R-R interval time series resulted in a constant interval between points, and the FFT was performed. The area of each respective band was used to calculate Hf HRV (0.15 – 0.40 Hz) and Lf HRV (0.04 – 0.15 Hz). An increase of Hf HRV and a decrease of Lf HRV/Hf HRV are indications of activation of parasympathetic activity and the deactivation of sympathetic activity [72].

The signals were then separated into three bins: 30 seconds before heating to represent the baseline, 30 seconds before the end of heating to represent max heating, and 30 seconds before the end of cooling for max cooling. The extracted parameters from each signal were averaged together for each bin. The ratio between the heating/cooling and the baseline measurements represented the trend in the data.

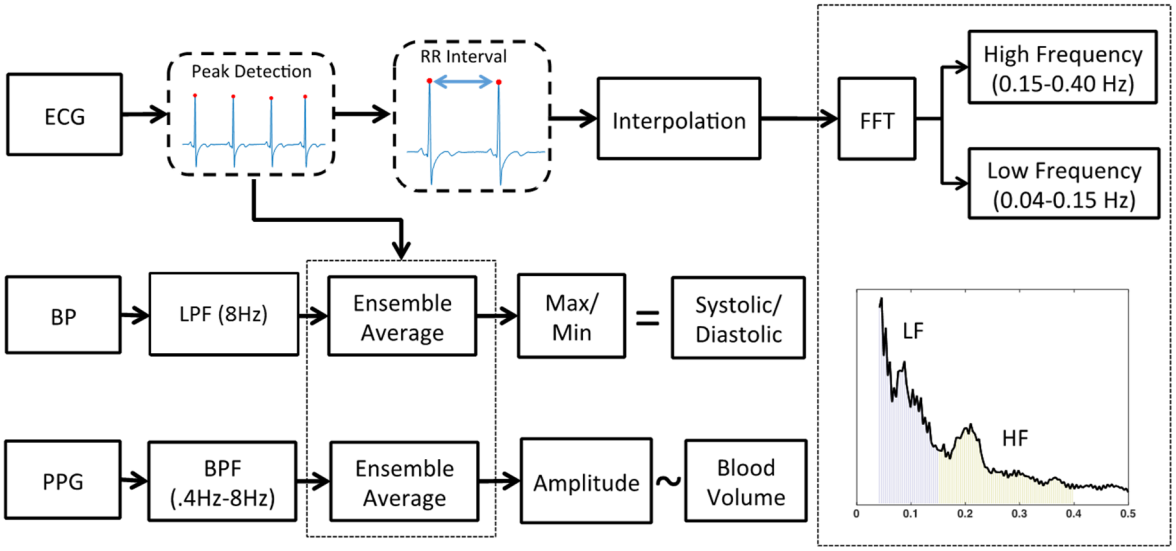

Figure 19 – Signal processing block diagram.

CHAPTER 5. RESULTS AND DISCUSSION

The results of the experiments are summarized in Table 2, Table 3, and Table 4 with Table 3 detailing the changes in glove PPG amplitude (Glove PPG), opposite hand PPG amplitude (Opp. PPG), Hf HRV, Lf/Hf HRV, systolic BP (SBP) and diastolic BP (DBP) during heating. Table 4 shows these same features during cooling.

As can be seen in Table 2, there is significant variability from person to person in the baseline parameters, which is expected since each person will have a different baseline hemodynamic state. Accordingly, the analysis focuses on changes in parameters associated with the temperature modulation protocol rather than the absolute value of each parameter at the hot or cold states alone. Blood pressure measurements for subject 6 (indicated by [a]) were excluded in this analysis due to errors in the Finapres measurements that suggested physiologically impossible measurements. The value of these parameters reported during the heating and cooling phase were normalized to the baseline phase (measured value / baseline value).

Table 2 – Baseline Measurements

	Baseline					
	Glove PPG	***Opp. PPG***	***Hf HRV***	***Lf/Hf HRV***	***SBP***	***DBP***
1	1.55	1.55	4.89	0.98	130	80
2	3.12	3.13	2.52	1.23	114	70
3	3.30	3.30	2.77	1.46	105	61
4	3.26	3.26	3.27	1.20	120	69
5	2.67	2.67	2.26	1.49	104	68
6	2.50	2.50	2.57	1.17	109	62

Table 3 – Heating Modulations

	Heating (Normalized to Baseline)					
	Glove PPG	***Opp. PPG***	***Hf HRV***	***Lf/Hf HRV***	***SBP***	***DP***
1	1.71	1.57	0.73	1.10	0.98	1.04
2	1.19	1.14	0.51	1.05	0.99	1.02
3	1.00	1.08	0.91	0.89	0.98	1.08
4	1.05	1.08	0.89	1.07	0.99	0.99
5	1.21	1.32	0.84	1.02	0.97	.98
6	0.65	0.78	0.91	1.07	-[a]	-[a]
μ	1.14	1.16	0.80	1.04	0.98	1.02
σ	0.35	0.27	0.16	0.07	0.01	0.04

Table 4 – Cooling Modulations

	Cooling (Normalized to Baseline)					
	Glove PPG	***Opp. PPG***	***Hf HRV***	***Lf/Hf HRV***	***SBP***	***DP***
1	0.93	0.93	0.98	1.24	1.04	1.04
2	0.91	0.92	1.16	1.00	1.02	1.02
3	0.96	0.92	0.74	0.87	1.02	1.14
4	0.69	0.91	0.70	1.02	1.02	1.01
5	0.86	0.99	1.68	0.98	1.04	1.10
6	0.37	0.48	1.06	0.98	-[a]	-[a]
μ	0.79	0.86	1.05	1.01	1.03	1.06
σ	0.23	0.19	0.36	0.12	0.01	0.06

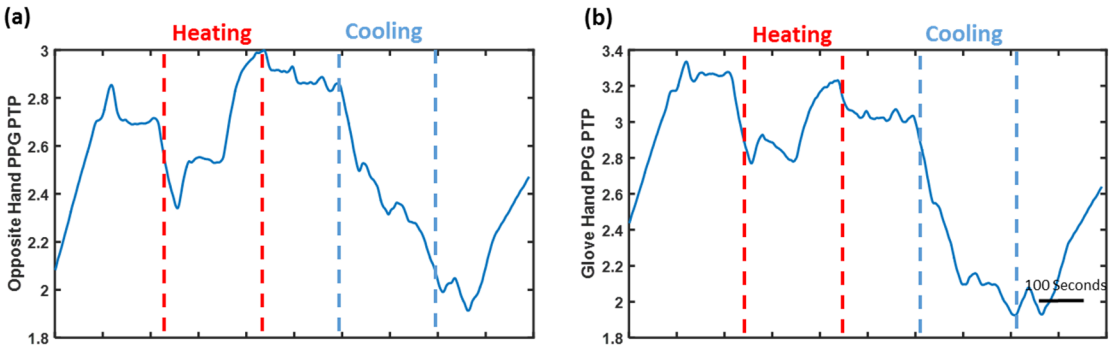

Figure 20 – PPG Amplitude of one subject for both the opposite hand (a) and the glove hand (b). During the heating phase, the amplitude of the signal increased, representing vasodilation. Cooling decreased this amplitude, indicating vasoconstriction.

During the heating phase, the amplitude of the glove PPG increased by an average of 14% ($p < 0.05$), indicating an increase in blood volume pulse to the hand and thus vasodilation. The opposite effect was found when cooling the hand, in which the PPG amplitude decreased for all subjects due to vasoconstriction. Figure 20 shows the amplitude of the PPG signal for a single subject during the testing. Since the temperature gradient was applied slowly, it is speculated that this response was dominated by the release of NO and not feedback from sensory nerves.

A change in Hf HRV and Lf/Hf HRV is an indication of the activation of a more central mechanism. Changes were seen during the heating intervention with the 20% decrease in Hf HRV ($p < 0.05$). Concurrently, Lf/Hf HRV increased in most of the subjects. These results indicate an increase in sympathetic activity and diminshed parasympathetic activity. Though Hf HRV has been shown in the existing literature to decrease during cold intervention with an increase in sympathetic tone, there were no consistent changes during this study. In addition, Lf/Hf HRV is expected to increase during cooling; however, no

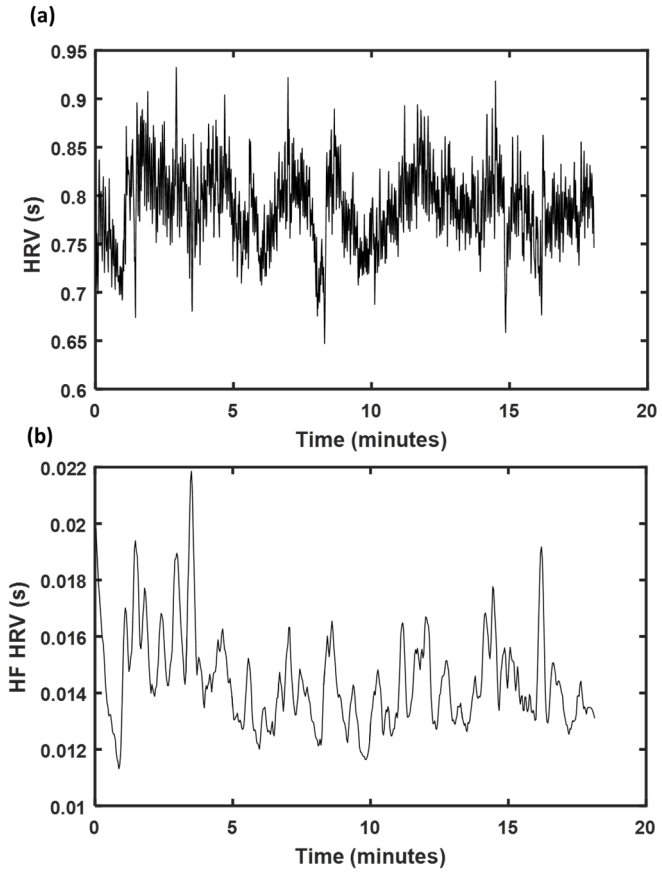

Figure 21 – Graphical representation of a subject during heating and cooling. (a) Raw R-R intervals. (b) The R-R intervals were interpolated and blocked off in 10 second intervals. The plot shows the energy of the high frequency band (.15-.4 Hz).

significant results were obtained during this study. The glove may not been able to create such a gradient to invoke a more central response, or this may be attributed to the small number of subjects that were studied in this proof-of-concept experiment. Variation in HRV may also be limited due to the lack of activation in the baroreflex during cooling.

The final parameters examined in this study, systolic and diastolic BP, both showed an increase during cooling ($p < 0.05$). Only systolic BP decreased during heating ($p < 0.05$). These changes are common in the literature for larger temperature gradients, such as with the cold pressor test involving the subject immersing his / her hand into a bucket of ice

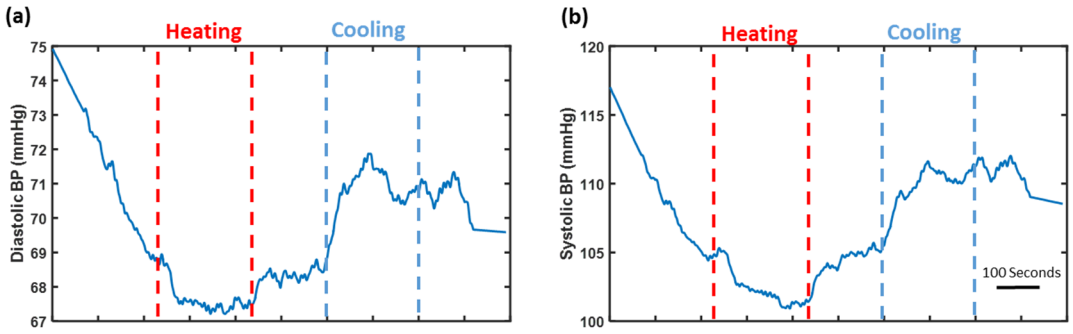

Figure 22 – Diastolic (a) and systalic (b) blood pressure measurements during heating and cooling. Heating slowly decreased blood pressure while cooling has an increased response in modulating blood pressure.

water [73]; however, to the best of our knowledge, an automated system with temperature control mechanisms built into the hardware has never previously been demonstrated as a means of modulating BP.

The use of this automatic temperature modulation protocol, and the associated analysis of the physiological changes, can serve to outline a "dose response" for the person to this particular perturbation. It is anticipated that changes in neuro-vascular health, or in resting autonomic state (for example, if a subject is stressed before beginning the protocol), can affect this dose response. If the glove were used in serial measurements, such as in the person's home, then changes to this dose response over time can be examined and possibly provide insight into early signs of microvascular dysfunction.

CHAPTER 6. CONCLUSION

The microvasculature plays a central role in mediating proper body functions. Degenerative and acute disorders can interfere with the delicate balance of physiological systems (endothelium, ANS, and VSM) involved in managing the microvasculature. However, current systems to assess this system's functions are bulky, expensive and require a medical professional to administer the test. Ultimately, they are not usable for longitudinal or at-home monitoring. The system described here can actively assess microvascular health by examining the responsivity of the vasculature to temperature stimuli. The system utilizes a feedback loop to strictly control the temperature of a glove with the intent of inducing a response. The glove was designed for potential at-home measurement, by incorporating no moving parts and simple controls.

The initial validation study evaluated the use of this temperature-controlled glove to apply local stimuli and examine the consistency of local and central physiological responses for healthy, young subjects. Significant changes were seen in both local blood flow and overall blood pressure during both heating and cooling, even with a small sample size ($n = 6$ subjects). Further work will include increasing the size of the subject population. Additionally, subjects with microvascular dysfunction will be included to compare the results and assess feasibility as a tool for outside-the-clinic monitoring.

REFERENCES

[1] W. COMMONS. (2007). *Cerebral angiography, arteria vertebralis sinister injection*.

[2] J. M. Johnson and D. L. Kellogg, "Local thermal control of the human cutaneous circulation," *Journal of Applied Physiology,* vol. 109, pp. 1229-1238, 2010-10-12 14:02:20 2010.

[3] M. Charakida, S. Masi, T. F. Lüscher, J. J. P. Kastelein, and J. E. Deanfield, "Assessment of atherosclerosis: the role of flow-mediated dilatation," *European Heart Journal,* vol. 31, pp. 2854-2861, 2010-12-01 12:02:47 2010.

[4] S. S. Segal, "Regulation of blood flow in the microcirculation," *Microcirculation,* vol. 12, p. 13, 20050404 DCOM- 20050802 2005.

[5] A. I. Vinik, T. S. Erbas T Fau - Park, K. K. Park Ts Fau - Pierce, K. B. Pierce Kk Fau - Stansberry, and K. B. Stansberry, "Methods for evaluation of peripheral neurovascular dysfunction," *Diabetes Technol Ther,* vol. 3, pp. 29-50, 2001.

[6] H. D. Critchley, "Neural mechanisms of autonomic, affective, and cognitive integration," *The Journal of Comparative Neurology,* vol. 493, pp. 154-166, 2005.

[7] C. Michiels, "Endothelial cell functions," *J Cell Physiol,* vol. 196, pp. 430-43, Sep 2003.

[8] L. Buée, P. R. Hof, C. Bouras, A. Delacourte, D. P. Perl, J. H. Morrison*, et al.*, "Pathological alterations of the cerebral microvasculature in Alzheimer's disease and related dementing disorders," *Acta Neuropathologica,* vol. 87, pp. 469-480, 1994.

[9] V. Schachinger, M. B. Britten, and A. M. Zeiher, "Prognostic impact of coronary vasodilator dysfunction on adverse long-term outcome of coronary heart disease," *Circulation,* vol. 101, pp. 1899-906, Apr 25 2000.

[10] M. C. Corretti, T. J. Anderson, E. J. Benjamin, D. Celermajer, F. Charbonneau, M. A. Creager*, et al.*, "Guidelines for the ultrasound assessment of endothelial-dependent flow-mediated vasodilation of the brachial artery: a report of the International Brachial Artery Reactivity Task Force," *J Am Coll Cardiol,* vol. 39, pp. 257-65, Jan 16 2002.

[11] A. J. Flammer, T. Anderson, D. S. Celermajer, M. A. Creager, J. Deanfield, P. Ganz*, et al.*, "The assessment of endothelial function: from research into clinical practice," *Circulation,* vol. 126, pp. 753-67, Aug 7 2012.

[12] K. binti Md Isa, N. Kawasaki, K. Ueyama, T. Sumii, and S. Kudo, "Effects of cold exposure and shear stress on endothelial nitric oxide synthase activation," *Biochemical and Biophysical Research Communications,* vol. 412, pp. 318-322, 8/26/ 2011.

[13] N. Charkoudian, "Skin blood flow in adult human thermoregulation: how it works, when it does not, and why," *Mayo Clin Proc,* vol. 78, pp. 603-12, May 2003.

[14] T. E. Wilson and C. G. Crandall, "Effect of Thermal Stress on Cardiac Function," *Exercise and sport sciences reviews,* vol. 39, pp. 12-17, 2011.

[15] M. I. K. Brenner, S. Thomas, and J. R. Shephard, "Spectral analysis of heart rate variability during heat exposure and repeated exercise," *European Journal of Applied Physiology and Occupational Physiology,* vol. 76, pp. 145-156, 1997.

[16] L. Mourot, M. Bouhaddi, and J. Regnard, "Effects of the cold pressor test on cardiac autonomic control in normal subjects," *Physiol Res,* vol. 58, pp. 83-91, 2009.

[17] H. L. Richardson, P. M. Macey, R. Kumar, E. M. Valladares, M. A. Woo, and R. M. Harper, "Neural and Physiological Responses to a Cold Pressor Challenge in Healthy Adolescents," *Journal of neuroscience research,* vol. 91, pp. 1618-1627, 09/16 2013.

[18] F. J. DiSalvo, "Thermoelectric Cooling and Power Generation," *Science,* vol. 285, p. 703, 1999.

[19] B. Alberts, A. Johnson, and J. Lewis, "Molecular biology of the cell," 4th ed. ed. New York :: Garland Science, 2002.

[20] P. Lacolley, V. Regnault, A. Nicoletti, Z. Li, and J.-B. Michel, "The vascular smooth muscle cell in arterial pathology: a cell that can take on multiple roles," *Cardiovascular Research,* vol. 95, p. 194, 2012.

[21] "SEER Training Modules, Classification & Structure of Blood Vessels," U. S. N. I. o. Health, Ed., ed. National Cancer Institute.

[22] "Marfan Syndrom," N. I. o. Health, Ed., ed. U.S. National Library of Medicine, 2016.

[23] D. L. Kellogg, "In vivo mechanisms of cutaneous vasodilation and vasoconstriction in humans during thermoregulatory challenges," *Journal of Applied Physiology,* vol. 100, p. 1709, 2006.

[24] P. M. Vanhoutte, "Endothelium and control of vascular function. State of the Art lecture," *Hypertension,* vol. 13, pp. 658-67, Jun 1989.

[25] T. W. Secomb, "Theoretical models for regulation of blood flow," *Microcirculation (New York, N.Y. : 1994),* vol. 15, pp. 765-775, 2008.

[26] P. C. Johnson, "Overview of the Microcirculation A2 - Tuma, Ronald F," in *Microcirculation (Second Edition)*, W. N. Durán and K. Ley, Eds., ed San Diego: Academic Press, 2008, pp. xi-xxiv.

[27] L. K. McCorry, "Physiology of the Autonomic Nervous System," *American Journal of Pharmaceutical Education,* vol. 71, p. 78, 11/27/received

[28] P. Low. *Overview of the Autonomic Nervous System*.

[29] G. D. Thomas, "Neural control of the circulation," *Advances in Physiology Education,* vol. 35, p. 28, 2011.

[30] M. P. Wiedeman, R. F. Tuma, and H. N. Mayrovitz, "5 - Factors Involved in the Regulation of Blood Flow," in *An Introduction to Microcirculation*, ed: Academic Press, 1981, pp. 99-139.

[31] D. L. Kellogg, P. E. Pérgola, K. L. Piest, W. A. Kosiba, C. G. Crandall, M. Grossmann*, et al.*, "Cutaneous Active Vasodilation in Humans Is Mediated by Cholinergic Nerve Cotransmission," *Circulation Research,* vol. 77, p. 1222, 1995.

[32] M. J. Fowler, "Microvascular and macrovascular complications of diabetes," *Clinical diabetes,* vol. 26, pp. 77-82, 2008.

[33] C. Popa, F. Popa, V. T. Grigorean, G. Onose, A. M. Sandu, M. Popescu*, et al.*, "Vascular dysfunctions following spinal cord injury," *Journal of Medicine and Life,* vol. 3, pp. 275-285, 08/25

[34] C. R. West, A. AlYahya, I. Laher, and A. Krassioukov, "Peripheral vascular function in spinal cord injury: a systematic review," *Spinal Cord,* vol. 51, pp. 10-19, 01//print 2013.

[35] V. T. Grigorean, A. M. Sandu, M. Popescu, M. Iacobini, R. Stoian, C. Neascu*, et al.*, "Vascular dysfunctions following spinal cord injury," *Journal of Medicine and Life,* vol. 3, pp. 275-285, 08/25

[36] J. C. Ramella-Roman and J. M. Hidler, *The Impact of Autonomic Dysreflexia on Blood Flow and Skin Response in Individuals with Spinal Cord Injury* vol. 2008, 2008.

[37] A. Krassioukov, D. E. R. Warburton, R. Teasell, J. J. Eng, and S. R. T. The, "A Systematic Review of the Management of Autonomic Dysreflexia Following Spinal Cord Injury," *Archives of physical medicine and rehabilitation,* vol. 90, pp. 682-695, 2009.

[38] C. A. Bauman, J. D. Milligan, F. J. Lee, and J. J. Riva, "Autonomic dysreflexia in spinal cord injury patients: an overview," *The Journal of the Canadian Chiropractic Association,* vol. 56, pp. 247-250, 2012.

[39] W. Young, "Spinal Cord Injury Levels & Classification," ed. Piscataway, NJ: W. M. Keck Center for Collaborative Neuroscience.

[40] W. T. Cade, "Diabetes-Related Microvascular and Macrovascular Diseases in the Physical Therapy Setting," *Physical Therapy,* vol. 88, pp. 1322-1335, 01/08/received

[41] J. E. Reusch, "Diabetes, microvascular complications, and cardiovascular complications: what is it about glucose?," *The Journal of clinical investigation,* vol. 112, pp. 986-988, 2003.

[42] A. Avogaro, M. Albiero, L. Menegazzo, S. de Kreutzenberg, and G. P. Fadini, "Endothelial Dysfunction in Diabetes," *Diabetes Care,* vol. 34, p. S285, 2011.

[43] M. Shea. *Cardiac Catherterization and Coronary Angiography*.

[44] A. L. Moens, I. Goovaerts, M. J. Claeys, and C. J. Vrints, "Flow-mediated vasodilation: a diagnostic instrument, or an experimental tool?," *Chest,* vol. 127, pp. 2254-63, Jun 2005.

[45] M. C. Corretti, T. J. Anderson, E. J. Benjamin, D. Celermajer, F. Charbonneau, M. A. Creager*, et al.*, "Guidelines for the ultrasound assessment of endothelial-dependent flow-mediated vasodilation of the brachial arteryA report of the International Brachial Artery Reactivity Task Force," *Journal of the American College of Cardiology,* vol. 39, pp. 257-265, 2002.

[46] C. I. Wright, C. I. Kroner, and R. Draijer, "Non-invasive methods and stimuli for evaluating the skin's microcirculation," *Journal of Pharmacological and Toxicological Methods,* vol. 54, pp. 1-25, 7// 2006.

[47] J. M. Johnson and D. W. Proppe, "Cardiovascular Adjustments to Heat Stress," in *Comprehensive Physiology*, ed: John Wiley & Sons, Inc., 2010.

[48] A. A. Romanovsky, "Skin temperature: its role in thermoregulation," *Acta Physiologica,* vol. 210, pp. 498-507, 2014.

[49] L. Walløe, "Arterio-venous anastomoses in the human skin and their role in temperature control," *Temperature: Multidisciplinary Biomedical Journal,* vol. 3, pp. 92-103, Jan-Mar

[50] H. Lenasi, *Assessment of Human Skin Microcirculation and Its Endothelial Function Using Laser Doppler Flowmetry*: INTECH Open Access Publisher, 2011.

[51] C. T. Minson, L. T. Berry, and M. J. Joyner, "Nitric oxide and neurally mediated regulation of skin blood flow during local heating," *Journal of Applied Physiology,* vol. 91, p. 1619, 2001.

[52] S. Earley, "Vanilloid and Melastatin Transient Receptor Potential Channels in Vascular Smooth Muscle," *Microcirculation (New York, N.Y. : 1994),* vol. 17, pp. 237-249, 2010.

[53] G. J. Hodges, W. A. Kosiba, K. Zhao, and J. M. Johnson, "The involvement of norepinephrine, neuropeptide Y, and nitric oxide in the cutaneous vasodilator response to local heating in humans," *Journal of Applied Physiology,* vol. 105, pp. 233-240, 05/15

[54] C. G. Crandall, B. D. Levine, and R. A. Etzel, "Effect of increasing central venous pressure during passive heating on skin blood flow," *J Appl Physiol (1985),* vol. 86, pp. 605-10, Feb 1999.

[55] C. G. Crandall, "Heat Stress and Baroreflex Regulation of Blood Pressure," *Medicine and science in sports and exercise,* vol. 40, p. 2063, 2008.

[56] S. Brauchi, P. Orio, and R. Latorre, "Clues to understanding cold sensation: Thermodynamics and electrophysiological analysis of the cold receptor TRPM8," *Proceedings of the National Academy of Sciences of the United States of America,* vol. 101, pp. 15494-15499, October 26, 2004 2004.

[57] C. D. Johnson, D. Melanaphy, A. Purse, S. A. Stokesberry, P. Dickson, and A. V. Zholos, "Transient receptor potential melastatin 8 channel involvement in the regulation of vascular tone," *American Journal of Physiology - Heart and Circulatory Physiology,* vol. 296, p. H1868, 2009.

[58] A. D. Flouris, D. A. Westwood, I. B. Mekjavic, and S. S. Cheung, "Effect of body temperature on cold induced vasodilation," *European Journal of Applied Physiology,* vol. 104, p. 491, 2008// 2008.

[59] F. Yamazaki, R. Sone, K. Zhao, G. E. Alvarez, W. A. Kosiba, and J. M. Johnson, "Rate dependency and role of nitric oxide in the vascular response to direct cooling in human skin," *Journal of Applied Physiology,* vol. 100, p. 42, 2005.

[60] G. J. Hodges, K. Zhao, W. A. Kosiba, and J. M. Johnson, "The involvement of nitric oxide in the cutaneous vasoconstrictor response to local cooling in humans," *The Journal of Physiology,* vol. 574, pp. 849-857, 05/25

[61] F. Yamazaki, "Local ascorbate administration inhibits the adrenergic vasoconstrictor response to local cooling in the human skin," *Journal of Applied Physiology,* vol. 108, p. 328, 2010.

[62] J. Cui, M. Shibasaki, D. A. Low, D. M. Keller, S. L. Davis, and C. G. Crandall, "Heat stress attenuates the increase in arterial blood pressure during the cold pressor test," *Journal of Applied Physiology,* vol. 109, p. 1354, 2010.

[63] Q. Zhao, L. A. Bazzano, J. Cao, J. Li, J. Chen, J. Huang, *et al.*, "Reproducibility of Blood Pressure Response to the Cold Pressor Test: The GenSalt Study," *American Journal of Epidemiology,* vol. 176, pp. S91-S98, 12/16/received

[64] Mihalache, I. Flamaropol, F. S. Dumitru, L. Dobrescu, and D. Dobrescu, "Automated cooling control system through Peltier effect and high efficiency control using a DC-DC Buck converter," in *Semiconductor Conference (CAS), 2015 International*, 2015, pp. 281-284.

[65] X. F. Teng and Y. T. Zhang, "The effect of contacting force on photoplethysmographic signals," *Physiological Measurement,* vol. 25, p. 1323, 2004.

[66] A. John, "Photoplethysmography and its application in clinical physiological measurement," *Physiological Measurement,* vol. 28, p. R1, 2007.

[67] A. M. Carek, T. H, x00F, reyin, S. Hersek, and O. T. Inan, "Preliminary methods for wearable neuro-vascular assessment with non-invasive, active sensing," in *2015 37th Annual International Conference of the IEEE Engineering in Medicine and Biology Society (EMBC)*, 2015, pp. 3113-3116.

[68] K. H. Wesseling, "Finger arterial pressure measurement with Finapres," *Z Kardiol,* vol. 85 Suppl 3, pp. 38-44, 1996.

[69] R. Mukkamala, J. O. Hahn, O. T. Inan, L. K. Mestha, C. S. Kim, T. H*, et al.*, "Toward Ubiquitous Blood Pressure Monitoring via Pulse Transit Time: Theory and Practice," *IEEE Transactions on Biomedical Engineering,* vol. 62, pp. 1879-1901, 2015.

[70] (2016). *PWM vs. Direct Current*.

[71] D. Alter, "Thermoelectric Cooler Control Using a TMS320F2812 DSP and a DRV592 Power Amplifier," in *DSP Application Report - Semiconductor Group*, ed: Texas Instruments, 2003.

[72] M. Malik, "Heart Rate Variability," *Annals of Noninvasive Electrocardiology,* vol. 1, pp. 151-181, 1996.

[73] E. A. Hines, Jr. and G. E. Brown, "The cold pressor test for measuring the reactibility of the blood pressure: Data concerning 571 normal and hypertensive subjects," *American Heart Journal,* vol. 11, pp. 1-9.